NUREG/CR-2146, Vol. 2
HEDL-TME 83-8

DYNAMIC ANALYSIS TO ESTABLISH NORMAL SHOCK AND VIBRATION OF RADIOACTIVE MATERIAL SHIPPING PACKAGES

QUARTERLY PROGRESS REPORT
APRIL 1, 1981 - JUNE 30, 1981

Hanford Engineering Development Laboratory

S.R. Fields

Prepared for the U.S. Nuclear Regulatory Commission

DISCLAIMER

Portions of this document may be illegible in electronic image products. Images are produced from the best available original document.

Availability of Reference Materials Cited in NRC Publications

Most documents cited in NRC publications will be available from one of the following sources:

1. The NRC Public Document Room, 1717 H Street, N.W.
   Washington, DC 20555
2. The NRC/GPO Sales Program, U.S. Nuclear Regulatory Commission,
   Washington, DC 20555
3. The National Technical Information Service, Springfield, VA 22161

Although the listing that follows represents the majority of documents cited in NRC publications, it is not intended to be exhaustive.

Referenced documents available for inspection and copying for a fee from the NRC Public Document Room include NRC correspondence and internal NRC memoranda; NRC Office of Inspection and Enforcement bulletins, circulars, information notices, inspection and investigation notices; Licensee Event Reports; vendor reports and correspondence; Commission papers; and applicant and licensee documents and correspondence.

The following documents in the NUREG series are available for purchase from the NRC/GPO Sales Program: formal NRC staff and contractor reports, NRC-sponsored conference proceedings, and NRC booklets and brochures. Also available are Regulatory Guides, NRC regulations in the *Code of Federal Regulations*, and *Nuclear Regulatory Commission Issuances*.

Documents available from the National Technical Information Service include NUREG series reports and technical reports prepared by other federal agencies and reports prepared by the Atomic Energy Commission, forerunner agency to the Nuclear Regulatory Commission.

Documents available from public and special technical libraries include all open literature items, such as books, journal and periodical articles, and transactions. *Federal Register* notices, federal and state legislation, and congressional reports can usually be obtained from these libraries.

Documents such as theses, dissertations, foreign reports and translations, and non-NRC conference proceedings are available for purchase from the organization sponsoring the publication cited.

Single copies of NRC draft reports are available free upon written request to the Division of Technical Information and Document Control, U.S. Nuclear Regulatory Commission, Washington, DC 20555.

Copies of industry codes and standards used in a substantive manner in the NRC regulatory process are maintained at the NRC Library, 7920 Norfolk Avenue, Bethesda, Maryland, and are available there for reference use by the public. Codes and standards are usually copyrighted and may be purchased from the originating organization or, if they are American National Standards, from the American National Standards Institute, 1430 Broadway, New York, NY 10018.

GPO Printed copy price: $4.25

NUREG/CR--2146-Vol.2

DE83 015854

NUREG/CR-2146, Vol. 2
HEDL-TME 83-8
RT

DYNAMIC ANALYSIS TO ESTABLISH NORMAL SHOCK AND VIBRATION OF RADIOACTIVE-MATERIAL SHIPPING PACKAGES

QUARTERLY PROGRESS REPORT APRIL 1, 1981 - JUNE 30, 1981

Hanford Engineering Development Laboratory

Operated by Westinghouse Hanford Company
P.O. Box 1970 Richland, WA 99352
A Subsidiary of Westinghouse Electric Corporation

S.R. Fields

Manuscript Completed: April 1983
Date Published: July 1983

Prepared for
Division of Engineering Technology
Office of Nuclear Regulatory Research
U.S. Nuclear Regulatory Commission
Washington, DC 20555
NRC Fin No. B2263

NUREG/CR-2146, Vol. 2
HEDL-TME 83-8
RT

DYNAMIC ANALYSIS TO ESTABLISH NORMAL SHOCK AND VIBRATION OF RADIOACTIVE MATERIAL SHIPPING PACKAGES

Quarterly Progress Report

April 1, 1981 - June 30, 1981

S. R. Fields

ABSTRACT

The CARDS (Cask Rail Car Dynamic Simulator) model was modified to simulate the cask-rail car systems used in Tests 13, 16 and 18 of the series of rail car coupling tests conducted at the Savannah River Laboratories (SRL) in July and August of 1978. An assessment of how well CARDS simulates the behavior of these cask-rail car systems was made by comparing calculated and experimental values of four response variables. This completes the development and validation of the CARDS model.

ACKNOWLEDGMENT

I would like to acknowledge the excellent work of H. A. Carlson who assisted in the preparation of the various figures in which calculated and measured results are compared.

CONTENTS

	Page
Abstract	iii
Acknowledgment	iv
Figures	vi
Tables	viii
SUMMARY OF PROGRESS	1
INTRODUCTION	3
PROGRESS TO DATE	4
NOTICE OF ERRORS IN PREVIOUS REPORTS	5
1. DEVELOP DYNAMIC MODEL	5
2. DATA COLLECTION AND REDUCTION	6
3. VALIDATE MODEL	6
4. COLLECT PARAMETER DATA	13
5. PARAMETRIC AND SENSITIVITY ANALYSIS	13
6. INTERIM REPORT	13
REFERENCES	14
APPENDIX A - FIGURES	A-1
APPENDIX B - TABLES	B-1

FIGURES

Figure		Page
1	Morphological Space Representation of Cask-Rail Car Coupling Tests	A-3
2	Cask-Rail Car Configuration Used in Tests 3 and 18	A-4
3	Cask-Rail Car Configuration Used in Tests 10 and 11	A-5
4	Cask-Rail Car Configuration Used in Test 13	A-6
5	Cask-Rail Car Configuration Used in Test 16	A-7
6	Coupler Force vs Time During Impact of Cask-Rail Car with Four Hopper Cars Loaded with Ballast (Test 16 - Instrument 3)	A-8
7	Horizontal Force of Interaction Between Cask and Rail Car vs Time During Impact with Four Hopper Cars Loaded with Ballast (Test 16 - Instruments 27 and 28)	A-9
8	Horizontal Acceleration of the Cask-Rail Car During Impact with Four Hopper Cars Loaded with Ballast (Test 16 - Instrument 7: Filtered at 100 Hz)	A-10
9	Horizontal Acceleration of the Cask During Impact with Four Hopper Cars Loaded with Ballast (Test 16 - Instrument 8: Filtered at 100 Hz)	A-11
10	Vertical Acceleration of the Cask at the Far End During Impact with Four Hopper Cars Loaded with Ballast (Test 16 - Instrument 11: Filtered at 50 Hz)	A-12
11	Vertical Acceleration of the Cask at the Struck End During Impact with Four Hopper Cars Loaded with Ballast (Test 16 - Instrument 9: Filtered at 50 Hz)	A-13
12	Horizontal Tiedown Force vs Relative Displacement Between Cask and Rail Car (Test 16)	A-14
13	Stiffness Coefficient of Horizontal Component of Tiedowns vs Relative Displacement Between Cask and Rail Car (Test 16)	A-15
14	Coupler Force vs Time During Impact of Cask-Rail Car with Four Hopper Cars Loaded with Ballast (Test 13 - Instrument 3)	A-16

FIGURES

Figure		Page
15	Horizontal Force of Interaction Between Cask and Rail Car vs Time During Impact with Four Hopper Cars Loaded with Ballast (Test 13 - Instruments 27 and 28)	A-17
16	Horizontal Acceleration of the Cask-Rail Car During Impact with Four Hopper Cars Loaded with Ballast (Test 13 - Instrument 7: Filtered at 50 Hz)	A-18
17	Horizontal Acceleration of the Cask During Impact with Four Hopper Cars Loaded with Ballast (Test 13 - Instrument 8: Filtered at 100 Hz)	A-19
18	Vertical Acceleration of the Cask at the Far End During Impact with Four Hopper Cars Loaded with Ballast (Test 13 - Instrument 11: Filtered at 50 Hz)	A-20
19	Vertical Acceleration of the Cask at the Struck End During Impact with Four Hopper Cars Loaded with Ballast (Test 13 - Instrument 9: Filtered at 50 Hz)	A-21
20	Coupler Force vs Time During Impact of Cask-Rail Car with Four Hopper Cars Loaded with Ballast (Test 18 - Instrument 3)	A-22
21	Horizontal Force of Interaction Between Cask and Rail Car vs Time During Impact with Four Hopper Cars Loaded with Ballast (Test 18 - Instruments 27 and 28)	A-23
22	Horizontal Acceleration of the Cask-Rail Car During Impact with Four Hopper Cars Loaded with Ballast (Test 18 - Instrument 12: Filtered at 50 Hz)	A-24
23	Horizontal Acceleration of the Cask During Impact with Four Hopper Cars Loaded with Ballast (Test 18 - Instrument 8: Filtered at 100 Hz)	A-25
24	Vertical Acceleration of the Cask at the Far End During Impact with Four Hopper Cars Loaded with Ballast (Test 18 - Instrument 11: Filtered at 50 Hz)	A-26
25	Vertical Acceleration of the Cask at the Struck End During Impact with Four Hopper Cars Loaded with Ballast (Test 18 - Instrument 9: Filtered at 50 Hz)	A-27

TABLES

Table		Page
1	Summary of Configurations and Conditions of Completed Cask-Rail Car Coupling Tests	B-3

DYNAMIC ANALYSIS TO ESTABLISH NORMAL SHOCK AND VIBRATION OF RADIOACTIVE MATERIAL SHIPPING PACKAGES

Quarterly Progress Report

April 1, 1981 - June 30, 1981

SUMMARY OF PROGRESS

1. DEVELOP DYNAMIC MODEL

The development of the basic CARDS (Cask Rail Car Dynamic Simulator) model has been completed. During this reporting period, the basic model was modified to simulate the cask-rail car systems used in Tests 13, 16 and 18 of the series of rail car coupling tests conducted at the Savannah River Laboratories (SRL) in July and August of 1978. These modifications were supplemented with adjustments suggested by comparisons of calculated and experimentally measured values of the horizontal force of interaction between the cask and rail car. The modified model was then validated by comparing calculated and measured values of four additional response variables.

3. VALIDATE MODEL

The validation of the CARDS model was completed with the comparison of measured results from Tests 13, 16 and 18 with corresponding results calculated using the CARDS model. An assessment of how well CARDS simulates the behavior of the cask-rail car systems used in these tests was made by comparing calculated and measured values of the horizontal force of interaction between the cask and rail car, the horizontal acceleration of the rail car, the horizontal acceleration of the cask, the vertical acceleration of the cask at the far end, and the vertical acceleration of the cask at the struck end. The coupler force measured during these tests was used as the force of excitation causing the system simulated by CARDS to vibrate.

The simulations of Tests 13, 16 and 18 were initially guided by comparisons of measured and calculated values of the horizontal force of interaction for Test 16. Differences between the measured and calculated values of this force for Test 16 were attributed to horizontal slippage between the cask and the rail car that resulted in an energy loss to the system. When this energy loss or "slippage" was accounted for in the model by modifying the stiffnesses of the horizontal components of the cable tiedowns, good agreement between the measured and calculated values of the horizontal interaction force and the other four response variables was realized. When these modifications were applied, without change, to the simulation of the cask-rail car systems used in Tests 13 and 18, substantial reductions were realized in the differences between the measured and calculated values of the five response variables compared.

On the basis of the comparisons of measured and calculated results for Tests 3, 10, 11, 13, 16 and 18, it is concluded that the CARDS model is an acceptable tool for the prediction of the dynamic response of a cask-rail car system impacting a stationary train of cars at speeds up to 11 mph.

INTRODUCTION

The objective of this study is to determine the extent to which the shocks and vibrations experienced by radioactive material shipping packages during normal transport conditions are influenced by or are sensitive to various structural parameters of the transport system (i.e., package, package supports, and vehicle). The purpose of this effort is to identify those parameters that significantly affect the normal shock and vibration environments so as to provide the basis for determining the forces transmitted to radioactive material packages. Determination of these forces will provide the input data necessary for a broad range of package-tiedown structural assessments.

Progress on this study from April 1, 1981 to June 30, 1981 will now be discussed. This is the last progress report in this series. The next report will be a final report summarizing the development and validation of the CARDS model, and the results of a parametric and sensitivity analysis using response spectra as figures of merit.

PROGRESS TO DATE

This study is divided into six tasks as discussed in previous progress reports. These previous progress reports are:

1. S. R. Fields, Dynamic Analysis to Establish Normal Shock and Vibration Environments Experienced by Radioactive Material Shipping Packages, NUREG/CR-0071, (HEDL-TME 78-19), Quarterly Progress Report (October 1 - December 31, 1977), Hanford Engineering Development Laboratory, May 1978.

2. S. R. Fields and S. J. Mech, Dynamic Analysis to Establish Normal Shock and Vibration of Radioactive Material Shipping Packages, NUREG/CR-0161, (HEDL-TME 78-41), Quarterly Progress Report (January 1 - March 31, 1978), Hanford Engineering Development Laboratory, July 1978.

3. S. R. Fields and S. J. Mech, Dynamic Analysis to Establish Normal Shock and Vibration of Radioactive Material Shipping Packages, NUREG/CR-0448, (HEDL-TME 78-74), Quarterly Progress Report (April 1 - June 30, 1978), Hanford Engineering Development Laboratory, December 1978.

4. S. R. Fields and S. J. Mech, Dynamic Analysis to Establish Normal Shock and Vibration of Radioactive Material Shipping Packages, NUREG/CR-0589, (HEDL-TME 78-102), Quarterly Progress Report (July 1 - September 30, 1978), Hanford Engineering Development Laboratory, March 1979.

5. S. R. Fields and S. J. Mech, Dynamic Analysis to Establish Normal Shock and Vibration of Radioactive Material Shipping Packages, NUREG/CR-0766, (HEDL-TME 79-3), Quarterly Progress Report (October 1 - December 31, 1978), Hanford Engineering Development Laboratory, June 1979.

6. S. R. Fields and S. J. Mech, Dynamic Analysis to Establish Normal Shock and Vibration of Radioactive Material Shipping Packages, NUREG/CR-0880, (HEDL-TME 79-29), Quarterly Progress Report (January 1 - March 31, 1979), Hanford Engineering Development Laboratory, July 1979.

7. S. R. Fields and S. J. Mech, Dynamic Analysis to Establish Normal Shock and Vibration of Radioactive Material Shipping Packages, NUREG/CR-1066, (HEDL-TME 79-43), Quarterly Progress Report (April 1 - June 30, 1979), Hanford Engineering Development Laboratory, October 1979.

8. S. R. Fields and S. J. Mech, Dynamic Analysis to Establish Normal Shock and Vibration of Radioactive Material Shipping Packages, NUREG/CR-1265, (HEDL-TME 79-71), Quarterly Progress Report (July 1 - September 30, 1979), Hanford Engineering Development Laboratory, March 1980.

9. S. R. Fields and S. J. Mech, Dynamic Analysis to Establish Normal Shock and Vibration of Radioactive Material Shipping Packages, NUREG/CR-1484, (HEDL-TME 80-24), Quarterly Progress Report (October 1 - December 31, 1979), Hanford Engineering Development Laboratory, August 1980.

10. S. R. Fields, Dynamic Analysis to Establish Normal Shock and Vibration of Radioactive Material Shipping Packages, NUREG/CR-1685, Volume 1, (HEDL-TME 80-51), Quarterly Progress Report (January 1 - March 31, 1980), Hanford Engineering Development Laboratory, January 1981.

11. S. R. Fields, Dynamic Analysis to Establish Normal Shock and Vibration of Radioactive Material Shipping Packages, NUREG/CR-1685, Volume 2, (HEDL-TME 80-72), Quarterly Progress Report (April 1 - June 30, 1980), Hanford Engineering Development Laboratory, April 1981.

12. S. R. Fields, Dynamic Analysis to Establish Normal Shock and Vibration of Radioactive Material Shipping Packages, NUREG/CR-1685, Volume 3, (HEDL-TME 80-91), Quarterly Progress Report (July 1 - September 30, 1980), Hanford Engineering Development Laboratory, April 1981.

13. S. R. Fields, Dynamic Analysis to Establish Normal Shock and Vibration of Radioactive Material Shipping Packages, NUREG/CR-1685, Volume 4, (HEDL-TME 80-92), Quarterly Progress Report (October 1 - December 31, 1980), Hanford Engineering Development Laboratory, July 1981.

14. S. R. Fields, Dynamic Analysis to Establish Normal Shock and Vibration of Radioactive Material Shipping Packages, NUREG/CR-2146, Volume 1, (HEDL-TME 81-15), Quarterly Progress Report (January 1 - March 31, 1981), Hanford Engineering Development Laboratory, November 1981.

NOTICE OF ERRORS IN PREVIOUS REPORTS

Errors were found in three of the above previously published quarterly reports. These reports are Volumes 2, 3 and 4 of NUREG/CR-1685 (HEDL-TME 80-72, HEDL-TME 80-91 and HEDL-TME 80-92, respectively). In these reports, all frequencies are angular frequencies and should be reported in units of radians/second rather than in units of Hz. This applies to all figures with frequency as the abscissa, and to all references to frequency in the texts of the reports.

1. DEVELOP DYNAMIC MODEL

The development of the basic CARDS (Cask Rail Car Dynamic Simulator) model has been completed. During this reporting period, the basic model was modified to simulate the characteristics of the cask-rail car systems used in Tests 13, 16 and 18 of the series of rail car coupling tests conducted at the Savannah River Laboratories (SRL) in July and August of 1978. These modifications were supplemented with adjustments suggested by comparisons of calculated and experimentally measured values of the horizontal force of interaction between the cask and rail car. These modifications and adjustments are discussed in detail in Section 3. VALIDATE MODEL.

2. DATA COLLECTION AND REDUCTION

This task has been completed.

3. VALIDATE MODEL

The validation of the CARDS model was completed with the comparison of measured results from Tests 13, 16 and 18, conducted at SRL in July and August of 1978, with corresponding results calculated using the CARDS model.

An assessment of how well the CARDS model simulates the behavior of the cask-rail car systems used in these tests was made by comparing calculated and measured values of the horizontal force of interaction between the cask and rail car, the horizontal acceleration of the rail car, the horizontal acceleration of the cask, the vertical acceleration of the cask at the far end, and the vertical acceleration of the cask at the struck end. The coupler force measured during these tests was used as the force of excitation causing the system simulated by CARDS to vibrate. This coupler force is shown in Figures 6, 14 and 20 for Tests 16, 13 and 18, respectively.

The cask used in Tests 13, 16 and 18 was the 40-ton Hallam cask used in Test 3 (see Figure 1, Table 1 and Reference 1). Unlike the box-shaped 70-ton cask used in Tests 10 and 11,[2] this cylindrical cask was mounted on and secured to a cradle structure that served as part of the tiedown structure. In Test 3, this cradle structure was fastened to a rail car with bolts; but, in Tests 13, 16 and 18, it was fastened to a different rail car (a different one for each of these three tests) with cables. As reported in Reference 1, good agreement between the calculated and experimental results for Test 3 was obtained only after allowance was made for slack in the vertical tiedown structure at the far end (opposite the struck end of the car). This slack, or looseness, in the tiedowns was evident in high speed films of Test 3. The films showed rain water being ejected from the collar at the far end of the cask at impact. Also, it was recalled that a rubber shim had been installed between the collar and the cask. When this gap and rubber shim combination was considered as part of the tiedown structure, and an appropriate non-linear stiffness coefficient devised, good agreement between the calculated and experimental results was obtained. This same non-linear representation of the stiffness coefficient for the vertical component of the rear tiedowns was used, without change, in the simulations of Tests 13, 16 and 18.

In Tests 10 and 11, the 70-ton cask was bolted directly to the rail car. As shown in Figure 1 and Table 1, the same rail car was used in Tests 3, 10 and 11. This rail car was a Seaboard Coastline (SCL) flat, bulkhead car with standard couplers. For Tests 13 and 16, an 80-ton flat rail car with three-wheeled trucks was used. The 80-ton rail car was equipped with a standard coupler on one end for use in Test 16, and a 15-inch travel end-of-car (EOC) cushion device on the opposite end for use in Test 13. This latter car is referred to as the 80-ton Union Carbide car because the Union Carbide Corporation converted it for transporting canisters placed in a welded, "saw-toothed" rack superstructure added to the top of the car.[3] For Test 18, a SCL flat bulkhead car with a cushion underframe coupling mechanism was used. The principal difference between this car and the one used in Tests 3, 10 and 11 was in the coupling mechanism used.[3]

The CARDS model is a complex two-dimensional, multi-degree-of-freedom model that determines the horizontal, vertical, and rotational motion of both the cask and its rail car following impact with an anvil train during coupling operations. Results of a parametric and sensitivity analysis, using CARDS and the cask-rail car configuration of Test 3, showed that the relative vertical and rotational accelerations (of the cask relative to the rail car) are highly sensitive and sensitive, respectively, to the horizontal distance between the centers-of-gravity (c.g.) of the cask and rail car.[4] This horizontal distance, given the parameter name l_{OCR} in Reference 4, is highlighted in Figures 2 through 5. Figures 2, 3, 4 and 5 are sketches of the cask-rail car configurations used in Tests 3 and 18, 10 and 11, 13, and 16, respectively. These figures identify not only l_{OCR} and the casks and rail cars used in the tests, but also the types of couplers and tiedowns used.

As stated earlier in Section 1, DEVELOP DYNAMIC MODEL, the simulations of Tests 13, 16 and 18 were initially guided by comparisons of measured and calculated values of the horizontal force of interaction between the cask and the rail car. In the CARDS model, this force is defined by the equation,

$$DUSLF = -(k_{S1} + k_{S4}) \left[(X_{RC} + Z_{RC}\theta_{RC}) - (X_P - Z_P\theta_P) \right] \qquad (1)$$

where:

DUSLF	= the horizontal interaction force, lb(force),
k_{S1} and k_{S4}	= stiffnesses of the horizontal components of the rear and front tiedowns, respectively, between the cask and rail car, lb(force)/inch,
X_{RC}	= the horizontal displacement of the c.g. of the cask-rail car, inches,
X_P	= the horizontal displacement of the c.g. of the cask or package, inches,
Z_{RC}	= the vertical distance from the horizontal centerline of the cask-rail car to its top and bottom surfaces, inches,
Z_P	= the vertical distance from the horizontal centerline of the cask to its top and bottom surfaces, inches,

θ_{RC} = the angle of the rotation of the X_{RC} and Y_{RC} axes about an axis peripendicular to the X_{RC} - Y_{RC} plane through the c.g. of the rail car, radians,

θ_P = the angle of rotation of the X_P and Y_P axes about an axis perpendicular to the X_P - Y_P plane through the c.g. of the cask or package, radians.

Initial comparisons revealed poor agreement between the calculated and measured values of this force. Specifically, after the peak forces following the impact pulses of Tests 13 and 16, the calculated results included some substantial negative values of this force while the measured results included only a few small negative values.

Of the three tests, Test 16 was the most similar to Test 3, a test simulated successfully earlier in the study (see Reference 1). The horizontal interaction force calculated for Test 3 did not show this tendency to negative values, so it was concluded that reasons for the differences in the results might be found by examining the differences in the cask-rail car systems used in these two tests. The primary differences between the cask-rail car systems of Test 3 and Test 16 are (see Figures 1, 2 and 5 and Table 1):

1) A 70-ton SCL flat, bulkhead rail car was used in Test 3. In Test 16 the 80-ton Union Carbide rail car was used. Both of these tests were conducted with standard couplers.

2) In Test 3, the c.g. of the cask was located 49.0 inches forward of the c.g. of the rail car. In Test 16, the c.g. of the cask was located 18.25 inches aft of the c.g. of the rail car (see Figures 2 and 5).

3) Bolted tiedowns were used for vertical restraint in Test 3. In Test 16, cable tiedowns were used.

The major difference between the cars used was in the car weights. The average weight of the loaded 80-ton Union Carbide car (designated as OROX805), based on weights measured prior to Tests 6 through 9 and Tests 12 through 16, is 160,105 lb. Only the 40-ton cask was used with this car, so subtracting the weight of this cask gives a car weight (which includes the cask cradle) of about 80,105 lb. The 70-ton SCL rail car used in Tests 1 through 5 and in Tests 10 and 11 was designated as ACL78498. The loaded weight of this car, measured prior to Tests 10 and 11, was 222,920 lb. Subtracting the weight of the 70-ton cask gives a car weight of about 82,920 lb. This means that the rail car used in Test 16 was about 3.4 percent lighter than the rail car used in Test 3. A lighter car would decelerate faster, resulting in less horizontal displacement of the car, i.e., X_{RC} in Equation (1) would be smaller. This would produce a greater tendency toward negative values of the horizontal interaction force; however, it was felt that the difference in the car weights was too small to account for the large negative values obtained from the model.

The location of the cask along the length of the rail car has little effect on the horizontal force of interaction. This is evident from the results of the parametric and sensitivity analysis reported in Reference 4. In Figures 91 and 92 of Reference 4, the horizontal distance between the vertical centerlines of the cask and rail car, l_{OCR}, is listed in the eighth and tenth positions, respectively, of ten parameters ranked according to their influence on the horizontal tiedown force. The only parameters ranked below l_{OCR} (that is, in positions indicating less influence) are the stiffness coefficients of the vertical components of the tiedowns, and two composite parameters representing variations of these coefficients.

The remaining difference between the cask-rail car systems of Tests 3 and 16 that might account for the differences in the calculated values of the horizontal interaction force is in the type of tiedowns used. The effect of the type of tiedowns used on the horizontal interaction force is primarily due to the stiffness coefficients of the horizontal components of the tiedowns [see Equation (1)]. It was reasoned that, because cables instead of bolts were used for vertical restraint in Test 16, the cask (and its cradle) apparently tended to shift longitudinally during impact and did not return to its original position. This was because the restoring "spring" action or "chocking" effect of the vertically oriented bolts was missing. Instead, energy was dissipated during the shifting of the cask.

The equations in the CARDS model that define the stiffness coefficients of the horizontal components of the tiedowns were modified to account for this loss of energy due to shifting of the cask. Previously, these stiffness coefficients were computed in a calculation sequence that set the coefficients either to their high or low values, or to the sum of their high and low values, depending upon conditions related to the movement of the cask (and its cradle). This procedure was retained, but the values computed were modified as follows. Let the unmodified values be expressed as

$$k_{S1} = f_1 \left[k_{S1}(\text{low}),\ k_{S1}(\text{high}) \right] \tag{2}$$

and

$$k_{S4} = f_4 \left[k_{S4}(\text{low}),\ k_{S4}(\text{high}) \right] \tag{3}$$

These coefficients were modified using the expressions

$$k_{S1}(\text{new}) = k_{S1}(\text{old}) \left[1 + M_{kS1} \text{Sgn} \left(\frac{dX_{RPRC}}{dt} \right) \right] \tag{4}$$

and

$$k_{S4}(\text{new}) = k_{S4}(\text{old}) \left[1 + M_{kS4} \text{Sgn} \left(\frac{dX_{RPRC}}{dt} \right) \right] \tag{5}$$

where:

$\frac{dX_{RPRC}}{dt}$ = the relative velocity of the cask-rail car combination, inches/second

$$= \frac{dX_P}{dt} - \frac{dX_{RC}}{dt},$$

$\frac{dX_P}{dt}$ = the velocity of the cask, inches/second,

$\frac{dX_{RC}}{dt}$ = the velocity of the rail car, inches/second,

M_{kS1}, M_{kS4} = Energy dissipation factors for k_{S1} and k_{S4}, respectively,

Sgn(A) = the sign function

$$= \begin{cases} +1, & A > 0 \\ -1, & A = 0 \\ -1, & A < 0 \end{cases} \quad \text{where } A = \frac{dX_{RPRC}}{dt}$$

The values of the energy dissipation factors used depend upon the conditions encountered and imposed, i.e.,

$$M_{kS1} = M_{kS1F} \qquad \left[\text{if } \frac{dX_{RPRC}}{dt} < 0 \text{ \underline{and} cable tiedowns used}\right] \qquad (6)$$

$$M_{kS1} = 0 \qquad [\text{otherwise}]$$

Similarly,

$$M_{kS4} = M_{kS4F} \qquad \left[\text{if } \frac{dX_{RPRC}}{dt} < 0 \text{ \underline{and} cable tiedowns used}\right] \qquad (7)$$

$$M_{kS4} = 0 \qquad [\text{otherwise}]$$

M_{kS1F} and M_{kS4F} are arbitrary factors currently set at 0.5.

The above representation of the stiffness coefficients in CARDS produced a good comparison of the calculated and measured values of the horizontal force of interaction between the cask and rail car of Test 16 (see Figure 7), and reasonable agreement in comparisons of four additional response variables (see Figures 8, 9, 10 and 11).

When the above equations and factors were used, without change, to determine the stiffness coefficients k_{S1} and k_{S4} for Tests 13 and 18, improvements in the comparisons of the calculated and measured results for these tests were also realized (see Figures 14 through 25).

The stiffness coefficients defined by Equations (4) and (5) generate hysteresis-type curves. Figure 12 is a load-deflection curve generated for the horizontal component of the tiedown at the far end during the simulation of Test 16, and Figure 13 is the corresponding plot of the stiffness coefficient k_{S1} as a function of the relative displacement X_P-X_{RC}.

Figure 8 shows three plots of the horizontal acceleration of the rail car during Test 16. The solid line is a plot of the calculated acceleration, the dashed line is a plot of the measured acceleration, and the dash-dot line is a plot of the calculated acceleration of the rail car with no cask. The calculated and measured values of the acceleration of the loaded rail car show poor agreement. During the peak pulse, the calculated acceleration is only about one-fourth the measured acceleration. The peak acceleration of the unloaded rail car is about one-half that of the measured acceleration during the same time period. There is strong evidence that suggests that the measured values of the acceleration may be in error. In Figure 3 of Reference 5, values of the horizontal acceleration of the loaded rail car, measured during Test 3, were compared with calculated values for both the loaded and unloaded rail car (an unloaded rail car is defined as one without both the cask and the trucks).

The purpose of this earlier comparison of results was to show that the horizontal motion of the cask strongly influences the horizontal motion of the rail car. These earlier comparisons showed that the calculated and measured results for the "loaded" system compare very well, and that the deceleration of the "isolated" or "unloaded" rail car is substantially greater. It was also shown that the deceleration of the unloaded car follows the coupler force curve. When the results in Figure 8 are compared with those of Figure 3 in Reference 5, the following facts may be noted:

1) The measured and calculated accelerations in Reference 5 are in very close agreement;

2) The peak calculated accelerations of both the loaded and unloaded rail cars in Figure 8 are consistent with those in Reference 5;

3) The calculated accelerations of the unloaded rail car, in Figure 8 and in Reference 5, follow the respective coupler force curves for Tests 16 and 3; and

4) The coupler force curves for Test 3 (see Figure 8 in Reference 1) and for Test 16 (see Figure 6) are not identical, but they are very similar and their peak values are in the neighborhood of 1.1×10^6 pounds force.

In addition to these facts, further evidence is suggested by the comparison of the measured and calculated values of the horizontal acceleration of the cask in Figure 9. This figure shows that very good agreement between the measured and calculated values was realized. It seems doubtful that such good agreement could be obtained for the horizontal acceleration of the cask while the measured and calculated values of the horizontal acceleration of the rail car show such poor agreement. It was shown earlier, in Reference 5, that the horizontal motion of the cask strongly influences the horizontal motion of the rail car.

Measured and calculated values of the vertical acceleration of the cask at the far end are compared in Figure 10. Only fair agreement was realized since the peak values of the calculated acceleration are about 50 or 60 percent greater than the measured accelerations, and the frequency is lower. However, the calculated results appear to be consistent with the corresponding results for Test 3 (see Figure 12 of Reference 1), while the measured results are about a factor of 2 less than those obtained from Test 3. The press of time ruled out an in-depth analysis of these differences that might have led to their verification or to some justification for modifications to the model that would have produced better agreement.

Figure 11 compares measured and calculated values of the vertical acceleration of the cask at the struck end. Here again, only fair agreement was realized. Comparisons with Test 3 results, in this case, do not show any resemblance or consistency. In fact, it appears that there is better agreement between the measured and calculated values for Test 16 than between corresponding values from Test 16 and Test 3. For example, the frequencies of both the measured and calculated values of Test 16 are higher than those of Test 3, and are consistent with one another. However, the frequency of the calculated results is higher than that of the measured results.

Although time did not permit an in-depth analysis to find a reason for the differences in the vertical accelerations of the cask obtained for the cask-rail car systems used in Tests 3 and 16, it should be pointed out again that one of the three primary differences between the cask-rail car systems used in these tests is the parameter l_{OCR}, the horizontal distance between the vertical centerlines of the cask and rail car. In Test 3, the c.g. of the cask was located 49.0 inches forward of the c.g. of the rail car whereas, in Test 16, the c.g. of the cask was located 18.25 inches aft of the c.g. of the rail car (see Figures 2 and 5). It is not certain what effect this has on the vertical accelerations, however, the results of the parametric and sensitivity analysis show that both the maximum absolute relative vertical acceleration of an equivalent single-degree-of-freedom model of the cask-rail car system of Test 3 and the maximum vertical acceleration of its support are highly sensitive to l_{OCR} (see Table 7 and Figures 86 and 89 of Reference 4).

It was stated earlier that when Equations (2) through (9) and the arbitrary factors M_{kS1F} and M_{kS4F} were used, without change, to determine the stiffness coefficients k_{S1} and k_{S4} for the cask-rail car systems used in Tests 13 and 18, improvements in the comparisons of the calculated and measured results for these tests were also realized. For these tests time did not permit further analysis beyond this stage; consequently, comparisons of measured and calculated values of response variables for these tests are presented, as developed, in Figures 15 through 25. Figures 15 through 25 show that, even though no further work was done, the calculated and measured results for these tests are in reasonable agreement.

Calculated and measured response variables for Test 3 have been compared in Reference 1, for Tests 10 and 11 in Reference 2, and for Tests 13, 16 and 18 in the present report. On the basis of these comparisons, it is concluded that the CARDS model is an acceptable tool for the prediction of the dynamic response of a cask-rail car system impacting a stationary train of cars at speeds up to 11 mph.

4. COLLECT PARAMETER DATA

This task has been completed.

5. PARAMETRIC AND SENSITIVITY ANALYSIS

This task has been completed.

6. INTERIM REPORT

No interim reports were published during this period.

REFERENCES

1. S. R. Fields, Dynamic Analysis to Establish Normal Shock and Vibration of Radioactive Material Shipping Packages, NUREG/CR-1685, Volume 2, (HEDL-TME 80-72), Quarterly Progress Report (April 1 - June 30, 1980), April 1981.

2. S. R. Fields, Dynamic Analysis to Establish Normal Shock and Vibration of Radioactive Material Shipping Packages, NUREG/CR-2146, Volume 1, (HEDL-TME 81-15), Quarterly Progress Report (January 1 - March 31, 1981), November 1981.

3. S. F. Petry, Rail Tiedown Tests with Heavy Casks for Radioactive Shipments, DP-1536, August 1980.

4. S. R. Fields, Dynamic Analysis to Establish Normal Shock and Vibration of Radioactive Material Shipping Packages, NUREG/CR-1685, Volume 4, (HEDL-TME 80-92), Quarterly Progress Report (October 1 - December 31, 1980), July 1981.

5. S. R. Fields, Dynamic Analysis to Establish Normal Shock and Vibration of Radioactive Material Shipping Packages, NUREG/CR-1685, Volume 1, (HEDL-TME 80-51), Quarterly Progress Report (January 1 - March 31, 1980), January 1981.

APPENDIX A

FIGURES

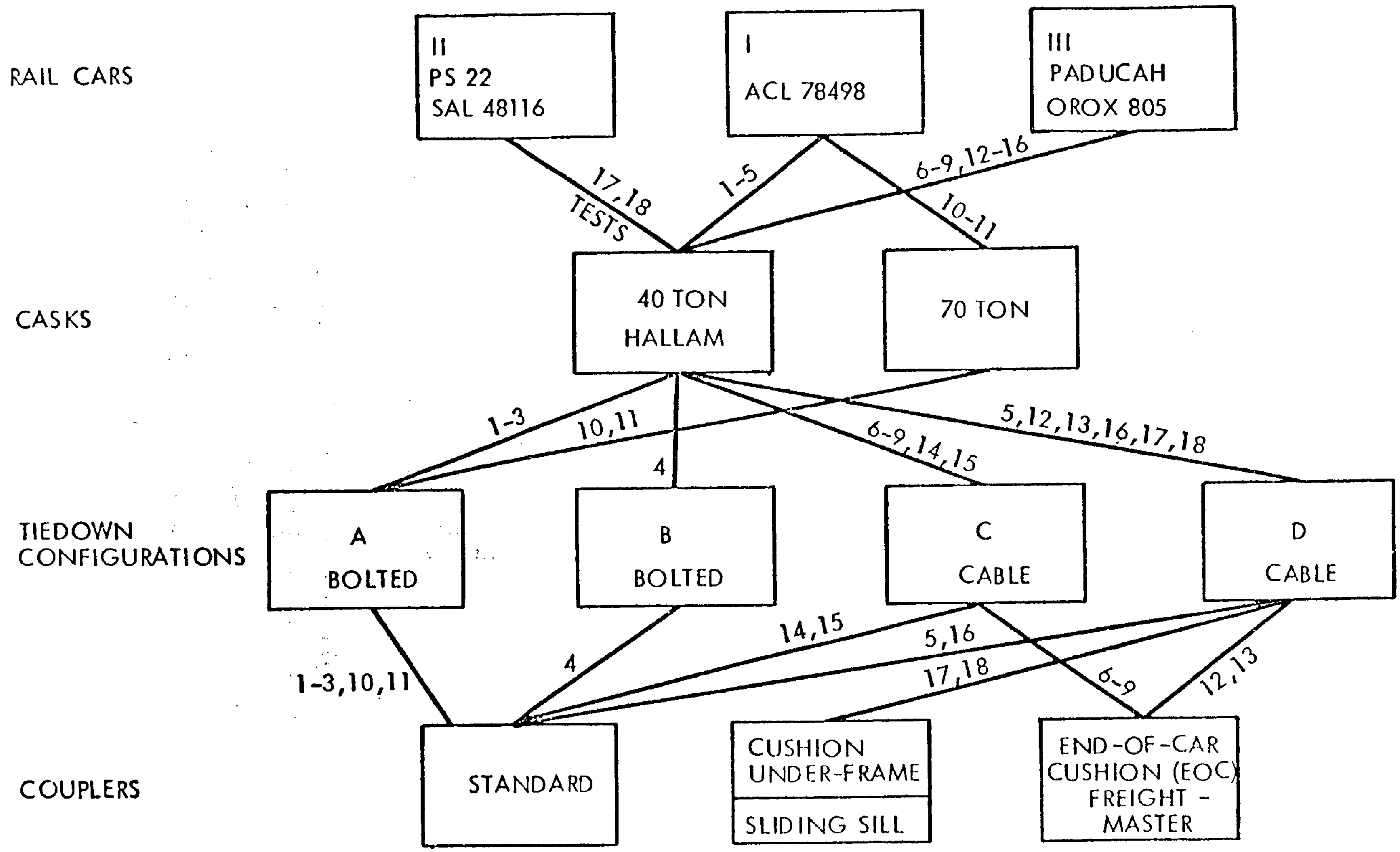

HEDL 7911-198.1

FIGURE 1. Morphological Space Representation of Cask-Rail Car Coupling Tests.

TESTS 3 AND 18

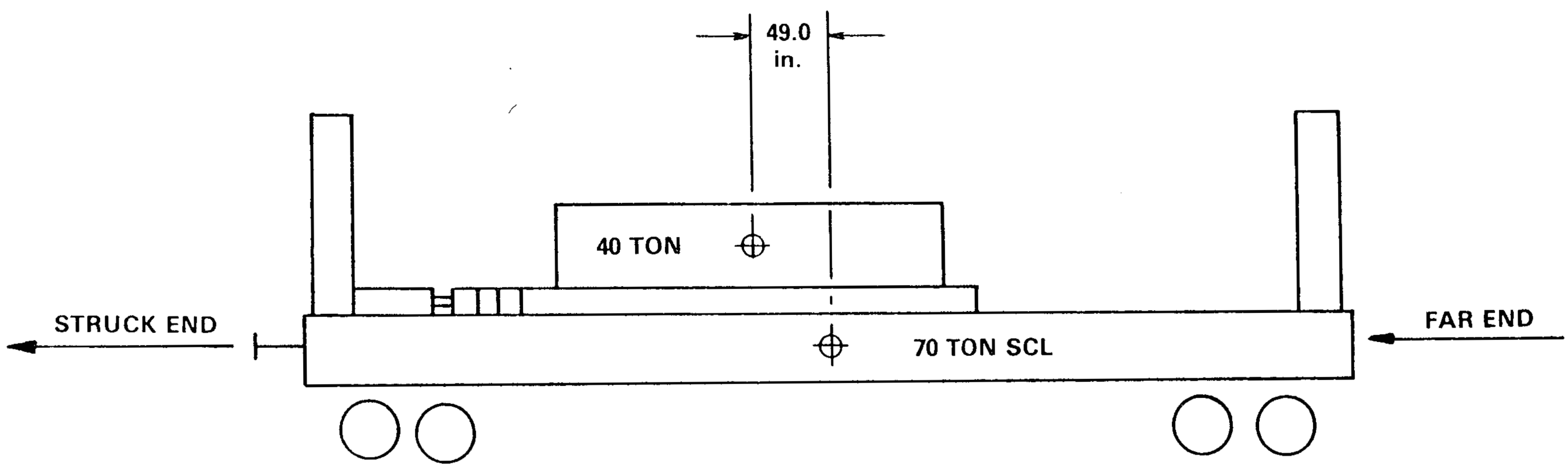

TEST 3
- STD DRAFT GEAR
- TIEDOWNS - 6 BOLTS
- P-22 RAIL CAR

TEST 18
- CUSHION UNDERFRAME
- TIEDOWNS - 6 CABLES
- PS-22 RAIL CAR

HEDL 8304-166.1

FIGURE 2. Cask-Rail Car Configuration Used in Tests 3 and 18.

TESTS 10 AND 11

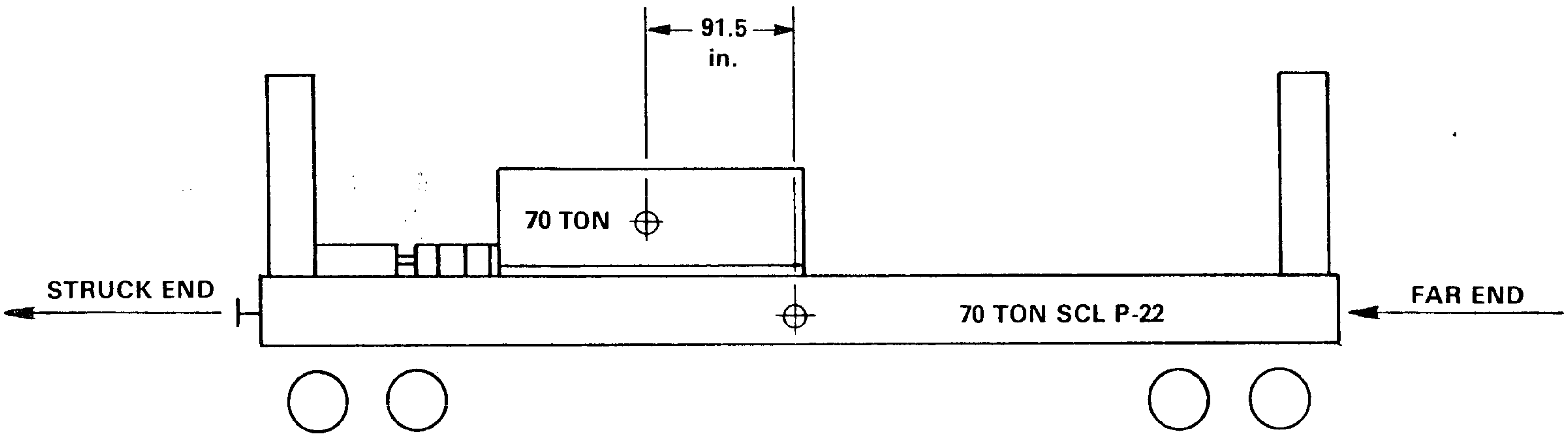

- STANDARD DRAFT GEAR
- TIEDOWNS - 6 BOLTS

HEDL 8304-166.2

FIGURE 3. Cask-Rail Car Configuration Used in Tests 10 and 11.

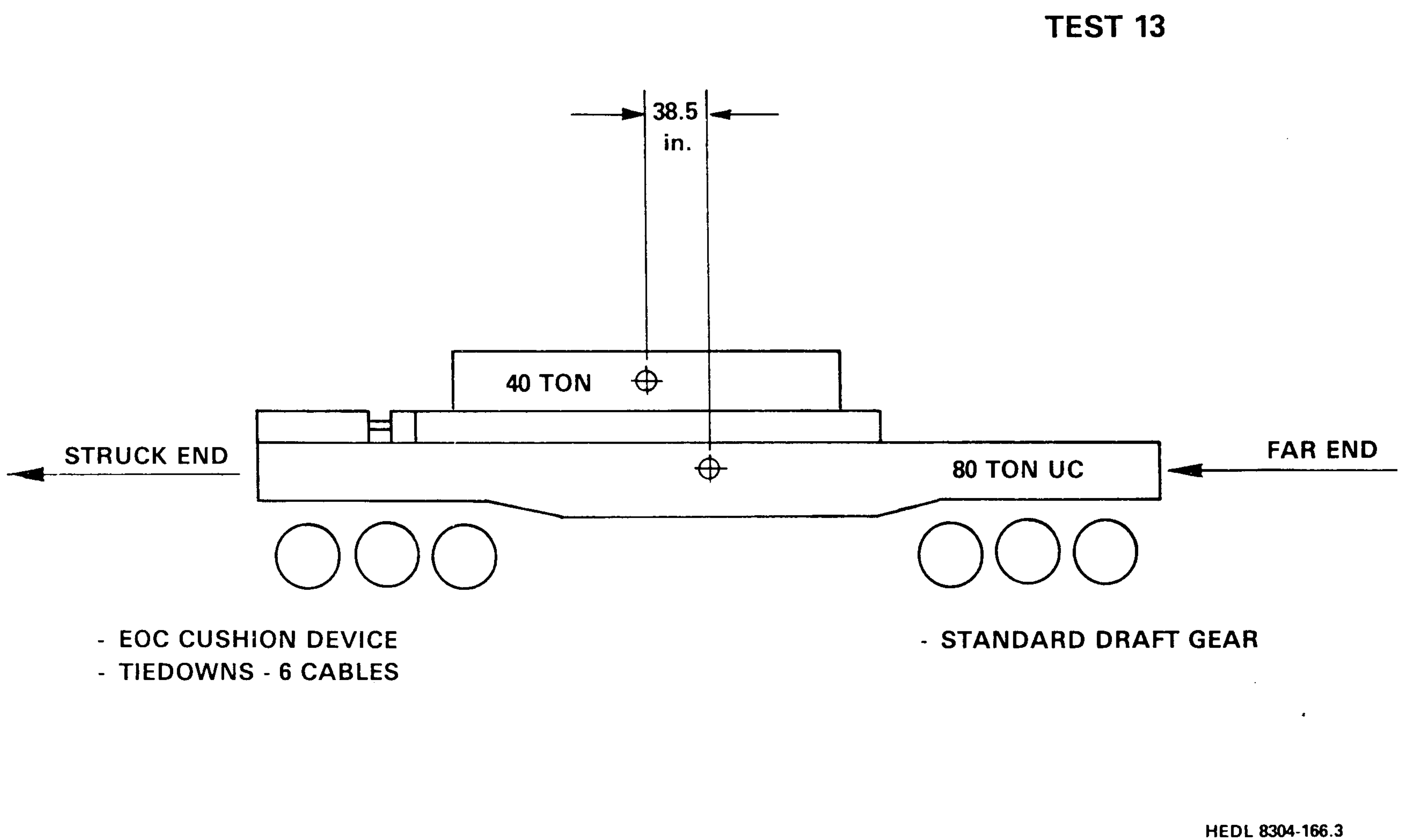

FIGURE 4. Cask-Rail Car Configuration Used in Test 13.

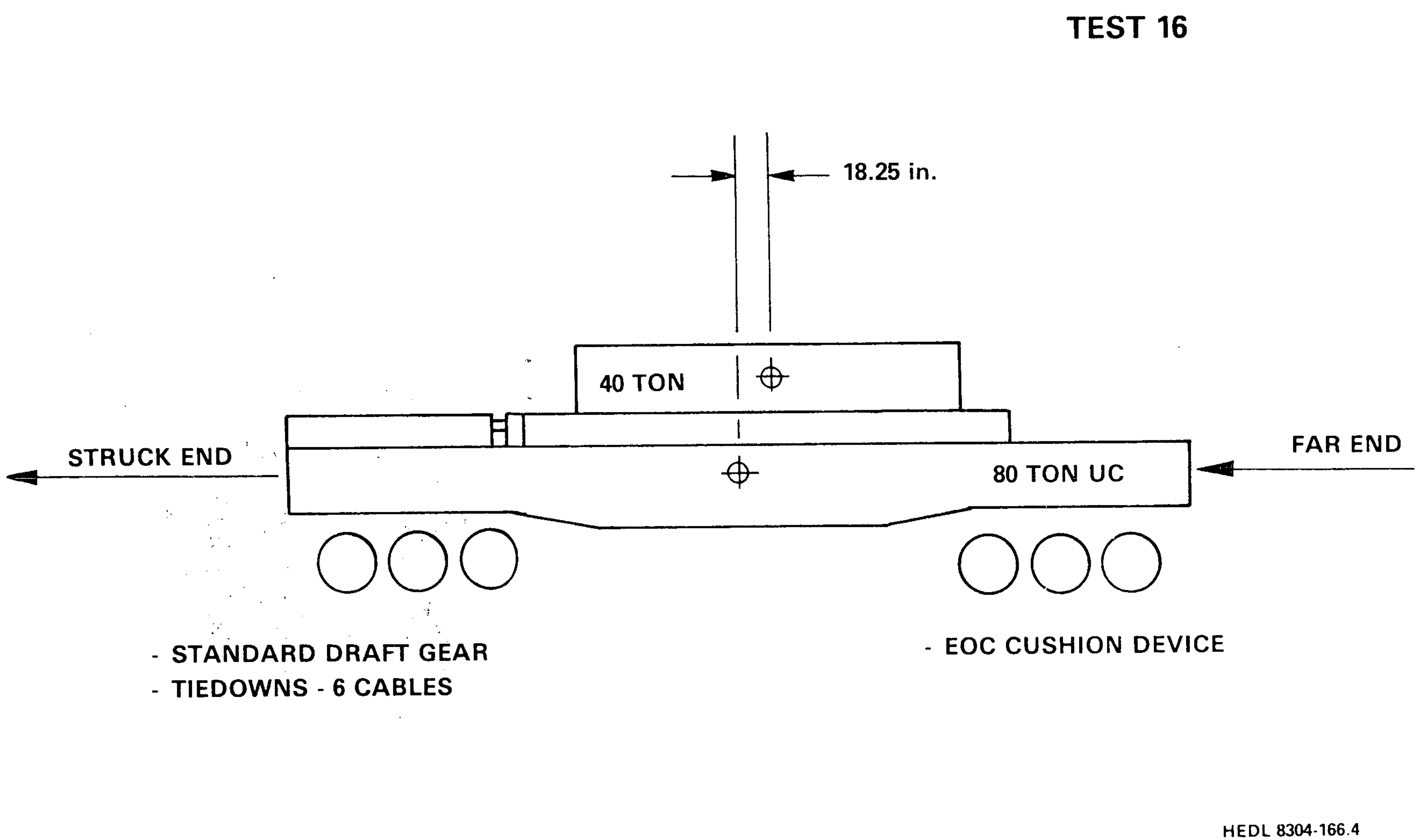

FIGURE 5. Cask-Rail Car Configuration Used in Test 16.

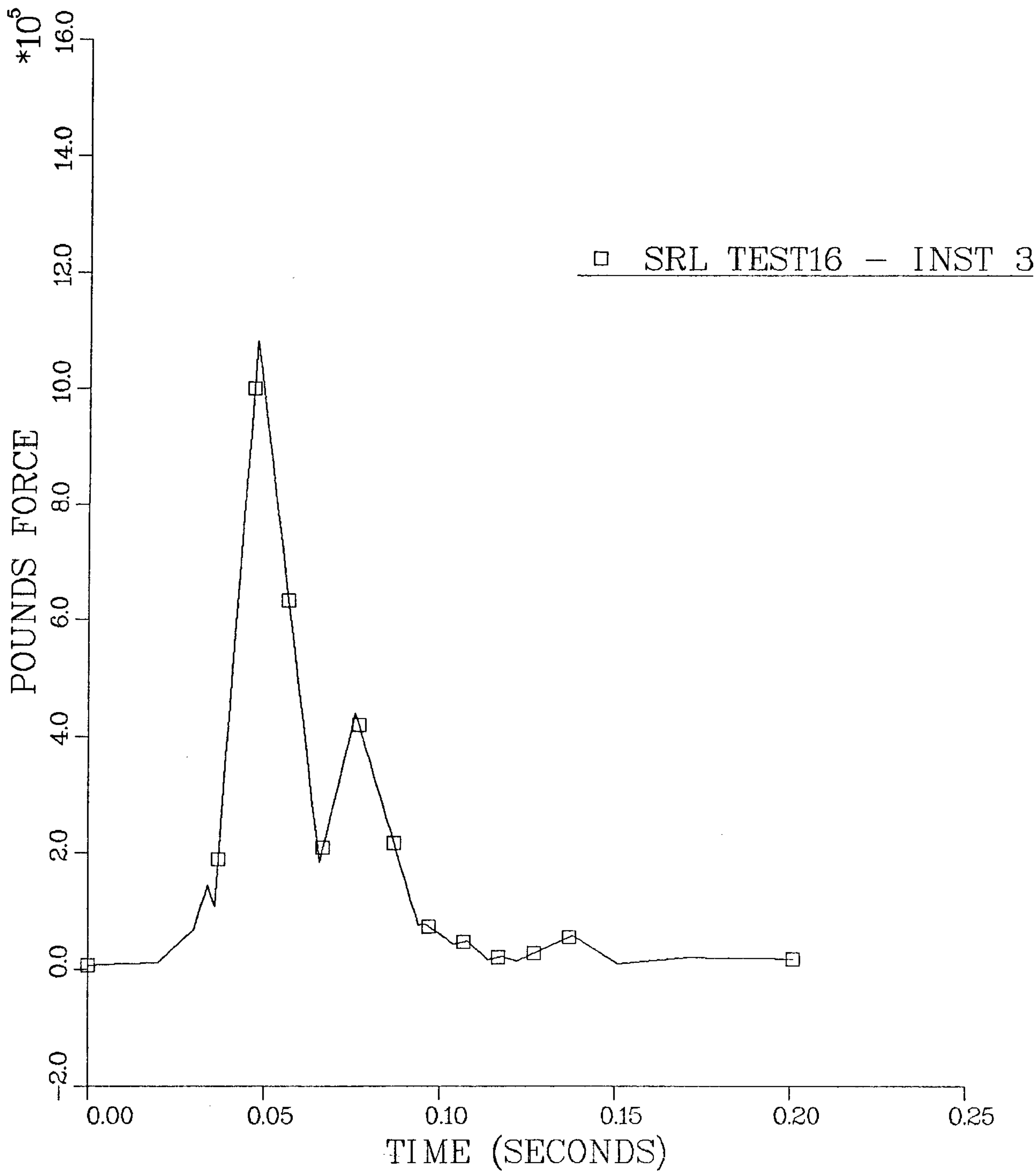

FIGURE 6. Coupler Force vs Time During Impact of Cask-Rail Car with Four Hopper Cars Loaded with Ballast (Test 16 - Instrument 3).

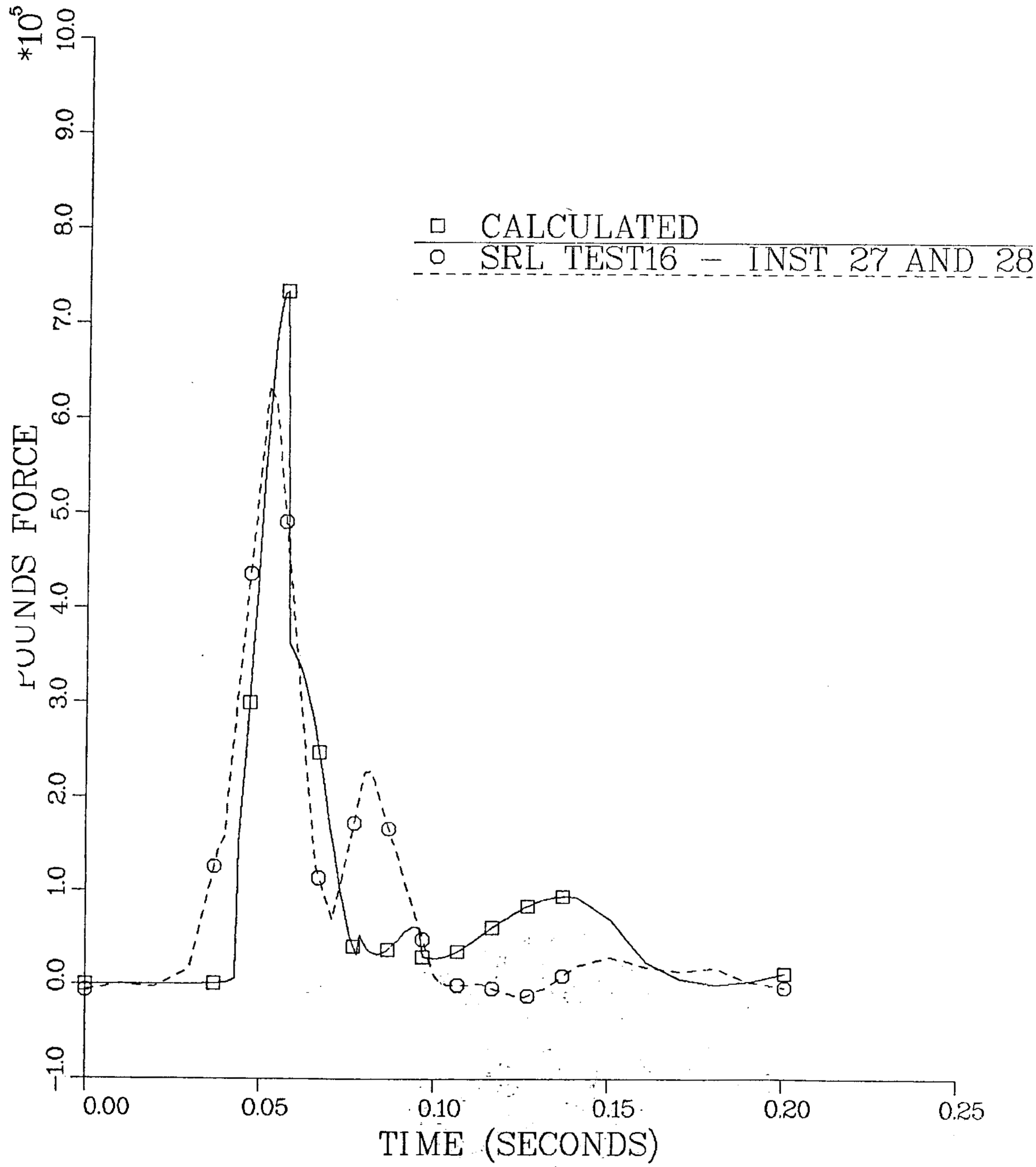

FIGURE 7. Horizontal Force of Interaction Between Cask and Rail Car vs Time During Impact with Four Hopper Cars Loaded with Ballast (Test 16 - Instruments 27 and 28).

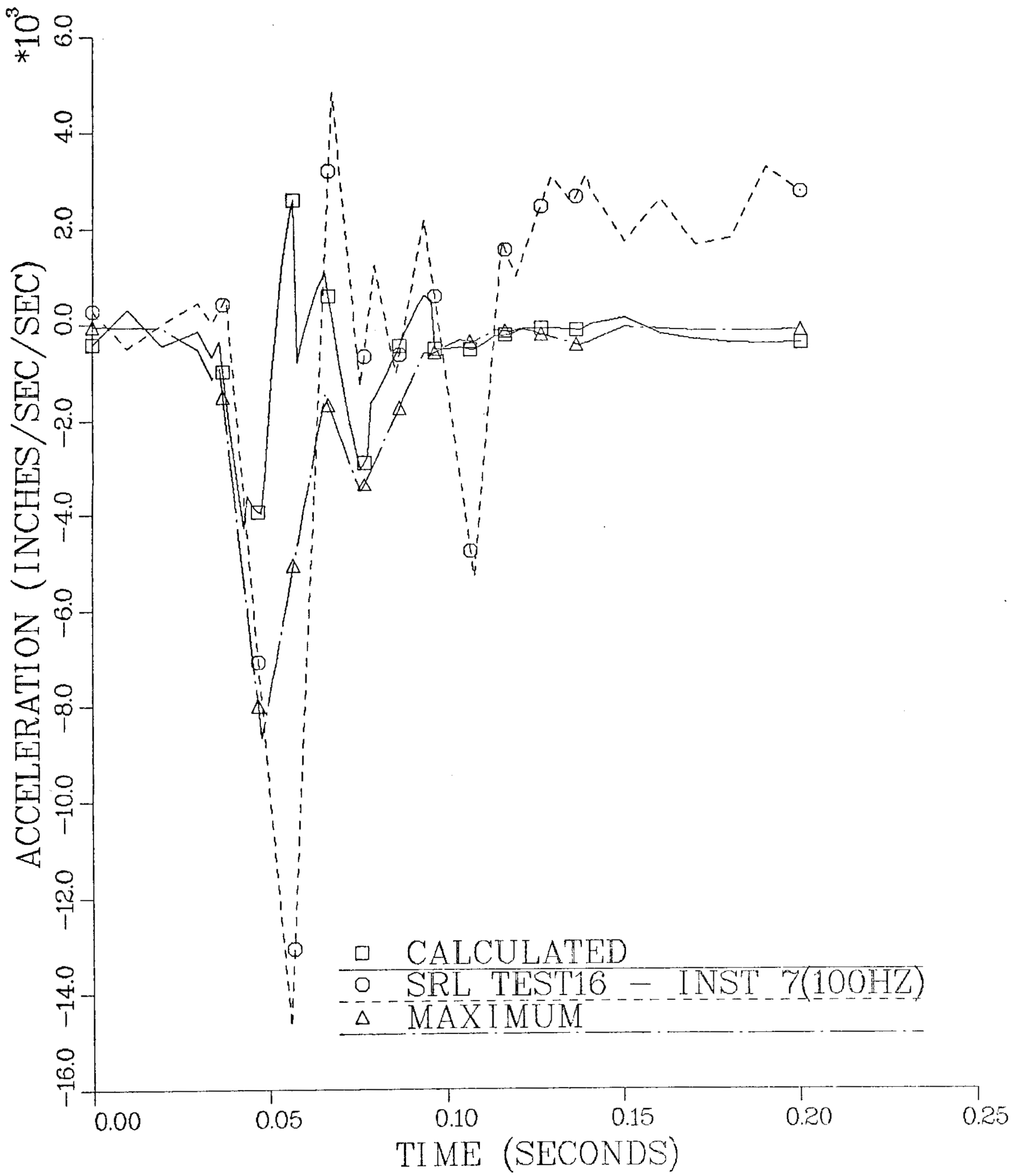

FIGURE 8. Horizontal Acceleration of the Cask-Rail Car During Impact with Four Hopper Cars Loaded with Ballast (Test 16 - Instrument 7: Filtered at 100 Hz).

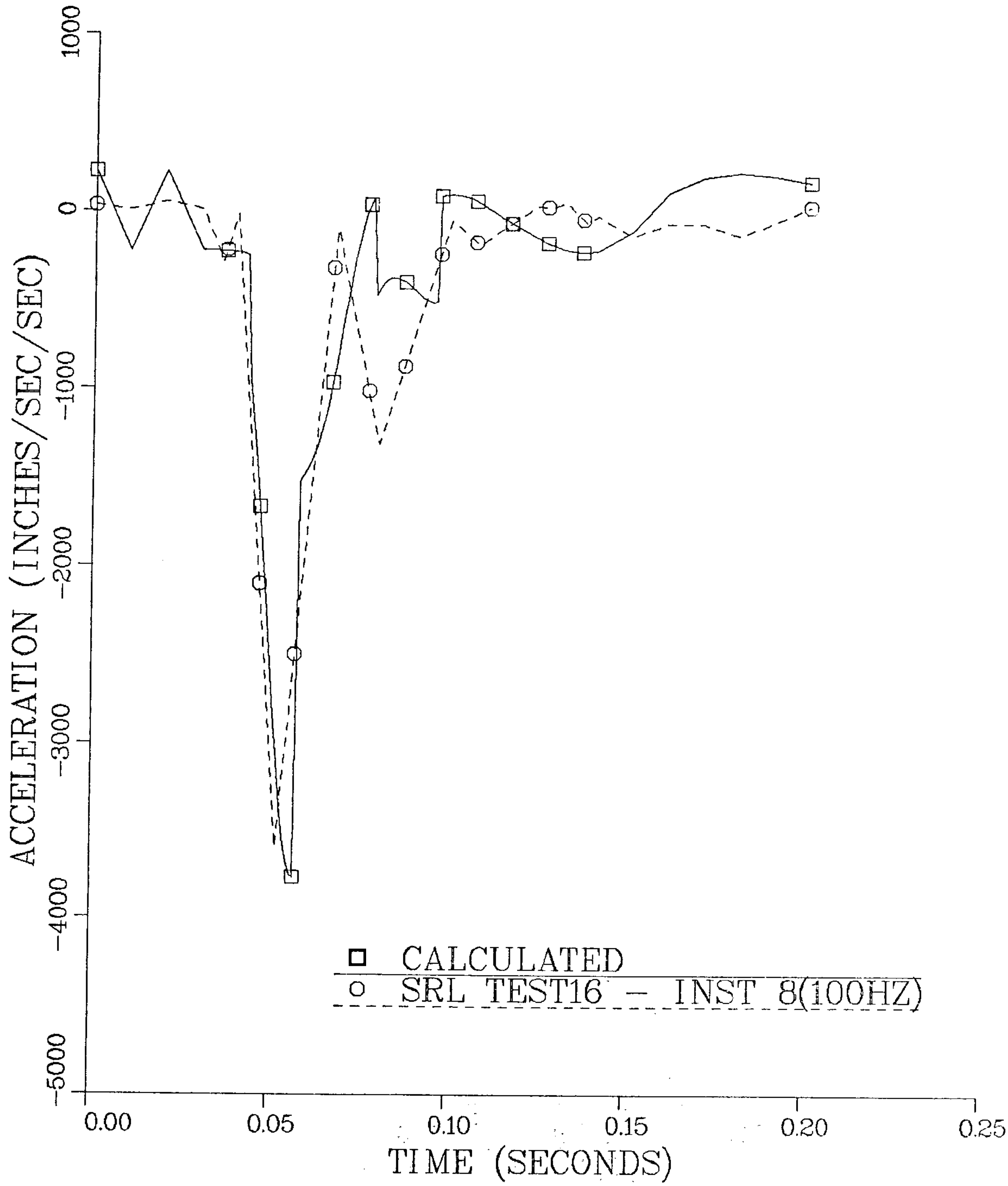

FIGURE 9. Horizontal Acceleration of the Cask During Impact with Four Hopper Cars Loaded with Ballast (Test 16 - Instrument 8: Filtered at 100 Hz).

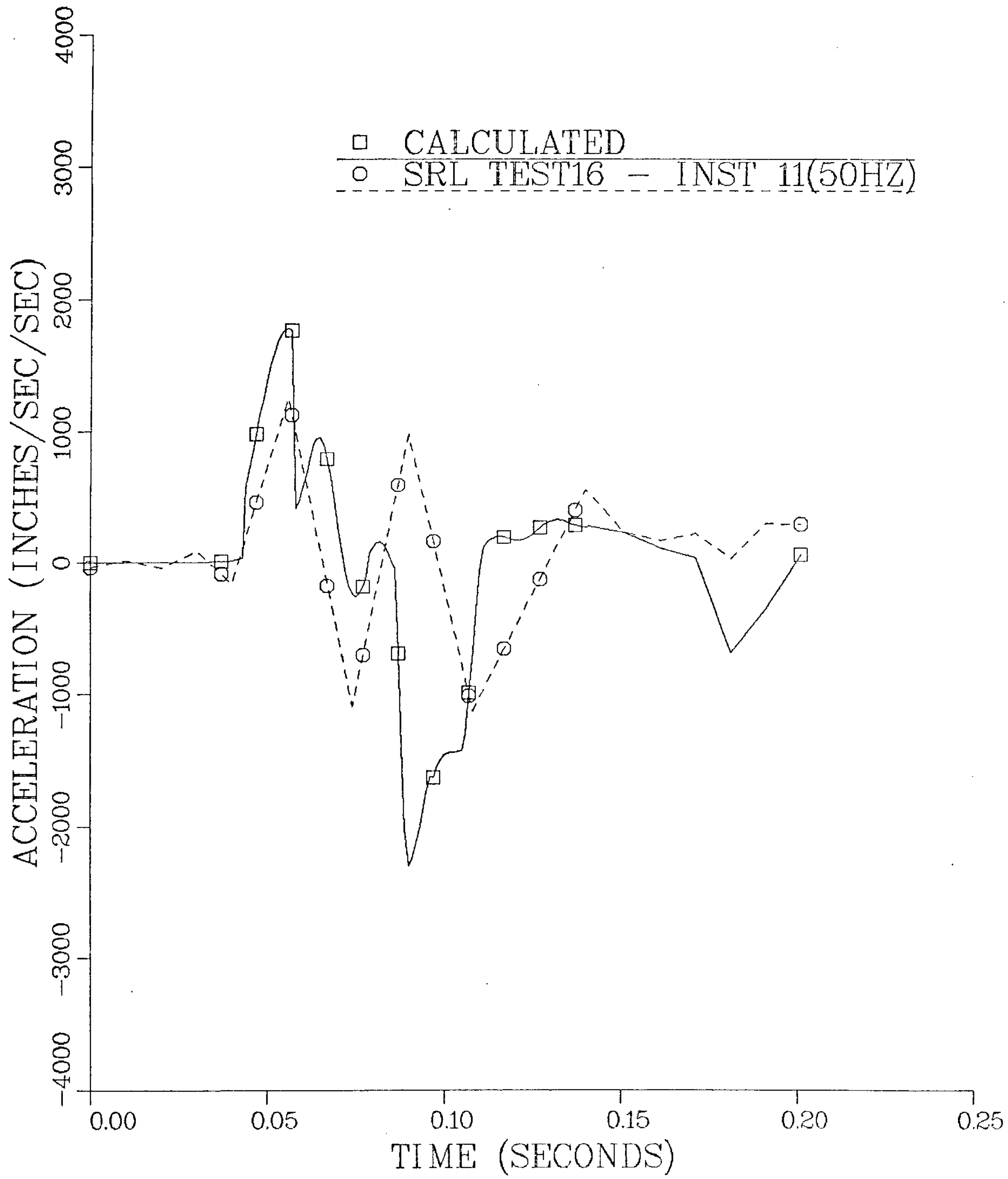

FIGURE 10. Vertical Acceleration of the Cask at the Far End During Impact with Four Hopper Cars Loaded with Ballast (Test 16 - Instrument 11: Filtered at 50 Hz).

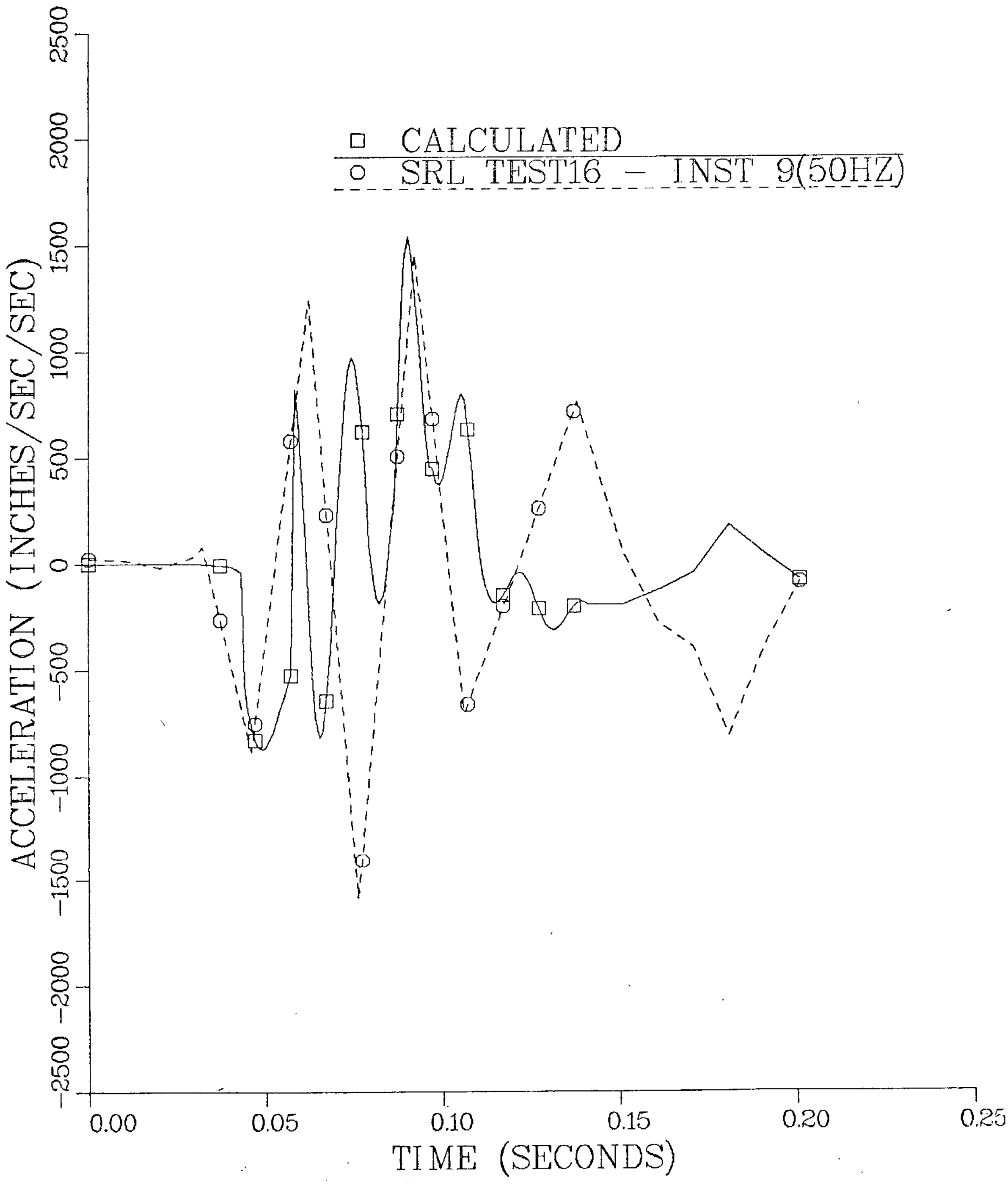

FIGURE 11. Vertical Acceleration of the Cask at the Struck End During Impact with Four Hopper Cars Loaded with Ballast (Test 16 - Instrument 9: Filtered at 50 Hz).

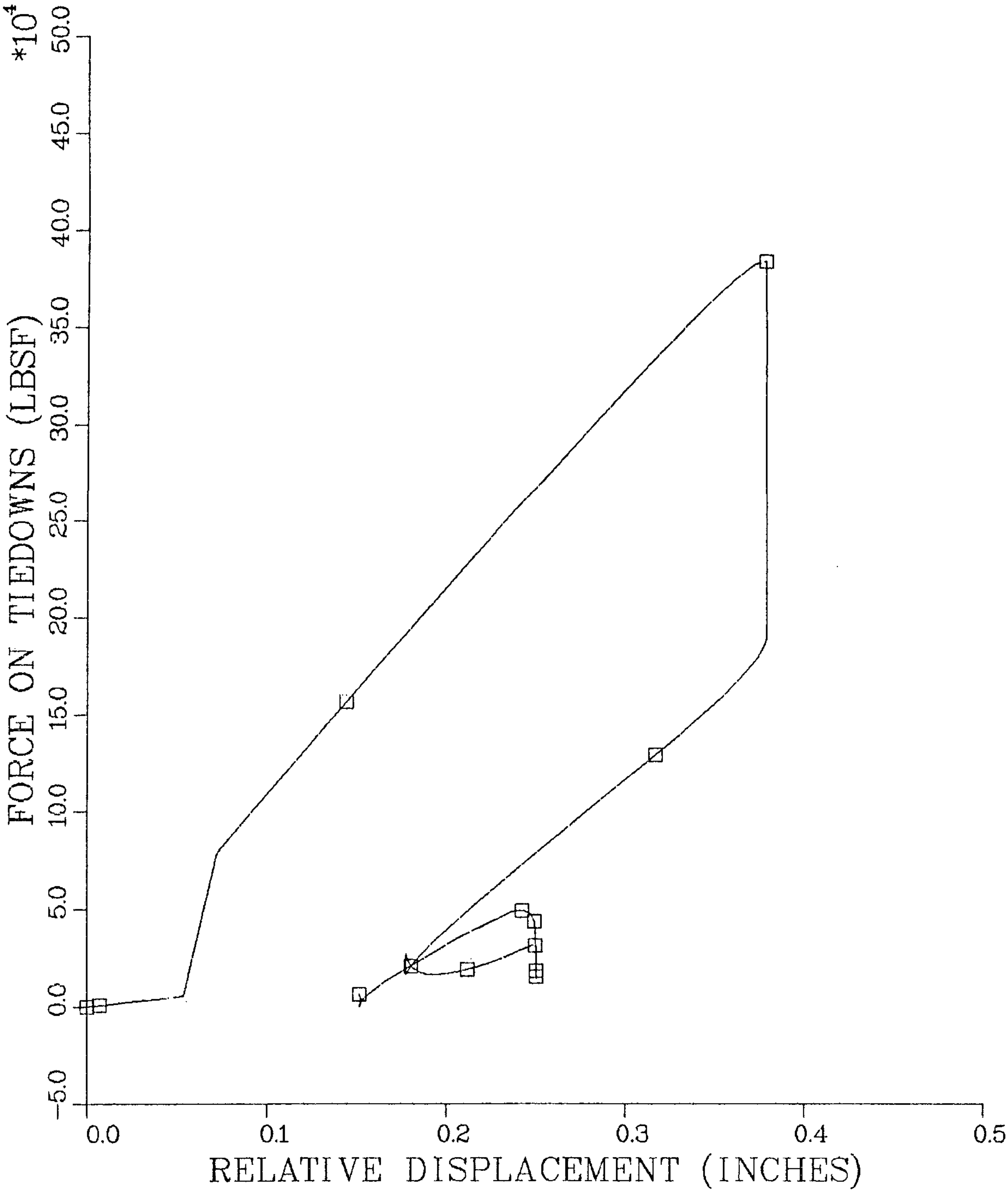

FIGURE 12. Horizontal Tiedown Force vs Relative Displacement Between Cask and Rail Car (Test 16).

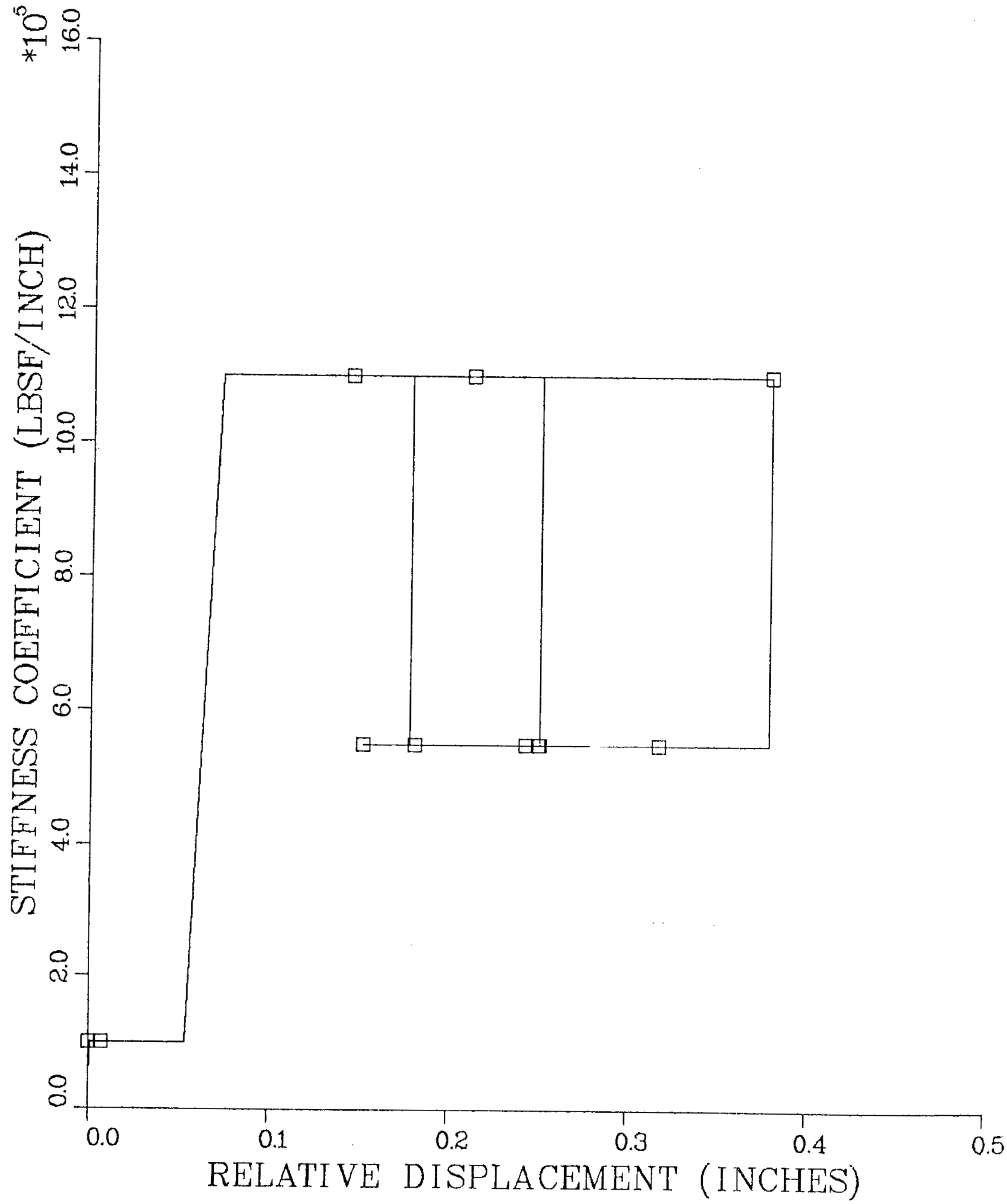

FIGURE 13. Stiffness Coefficient of Horizontal Component of Tiedowns vs Relative Displacement Between Cask and Rail Car (Test 16).

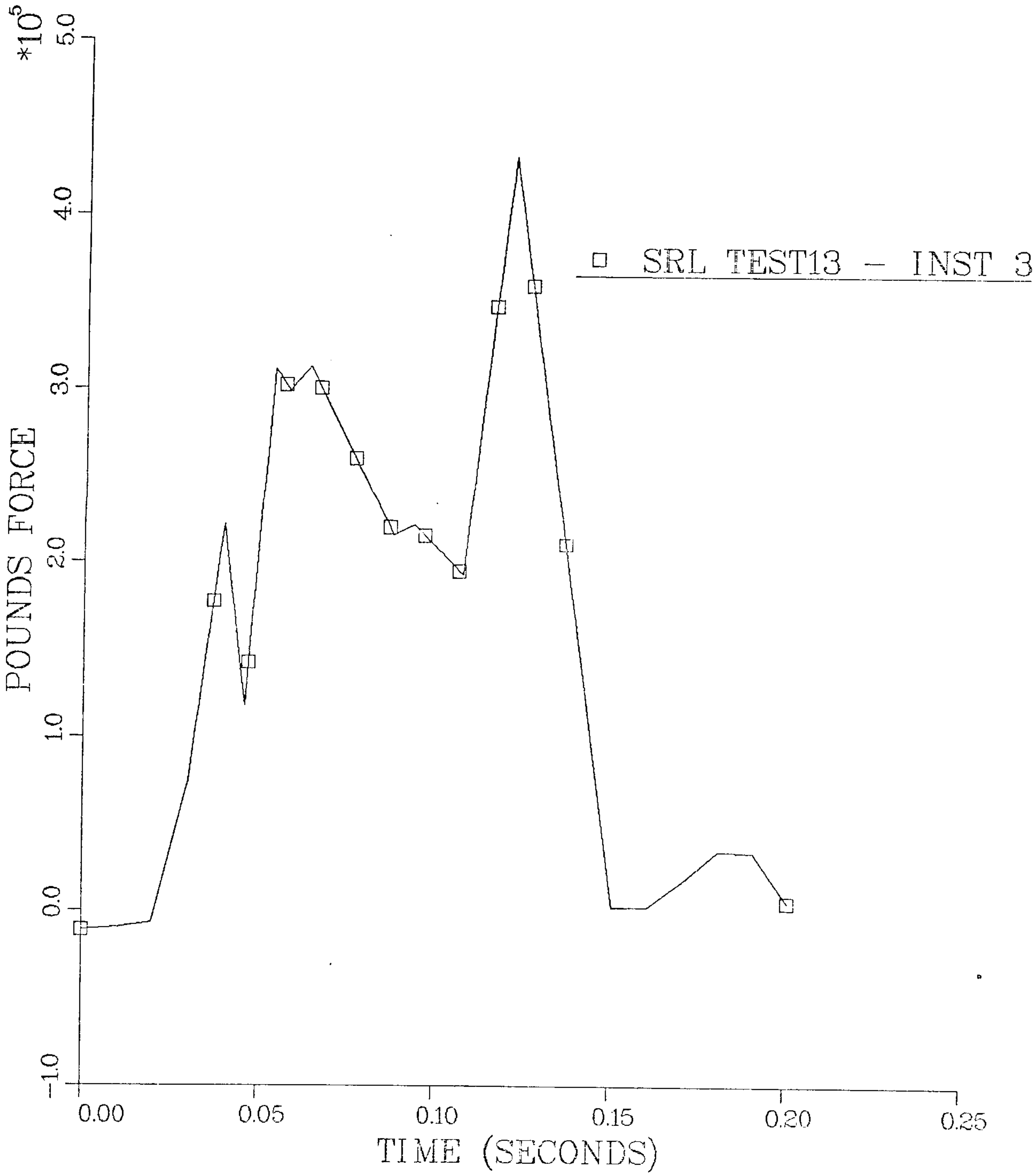

FIGURE 14. Coupler Force vs Time During Impact of Cask-Rail Car with Four Hopper Cars Loaded with Ballast (Test 13 - Instrument 3).

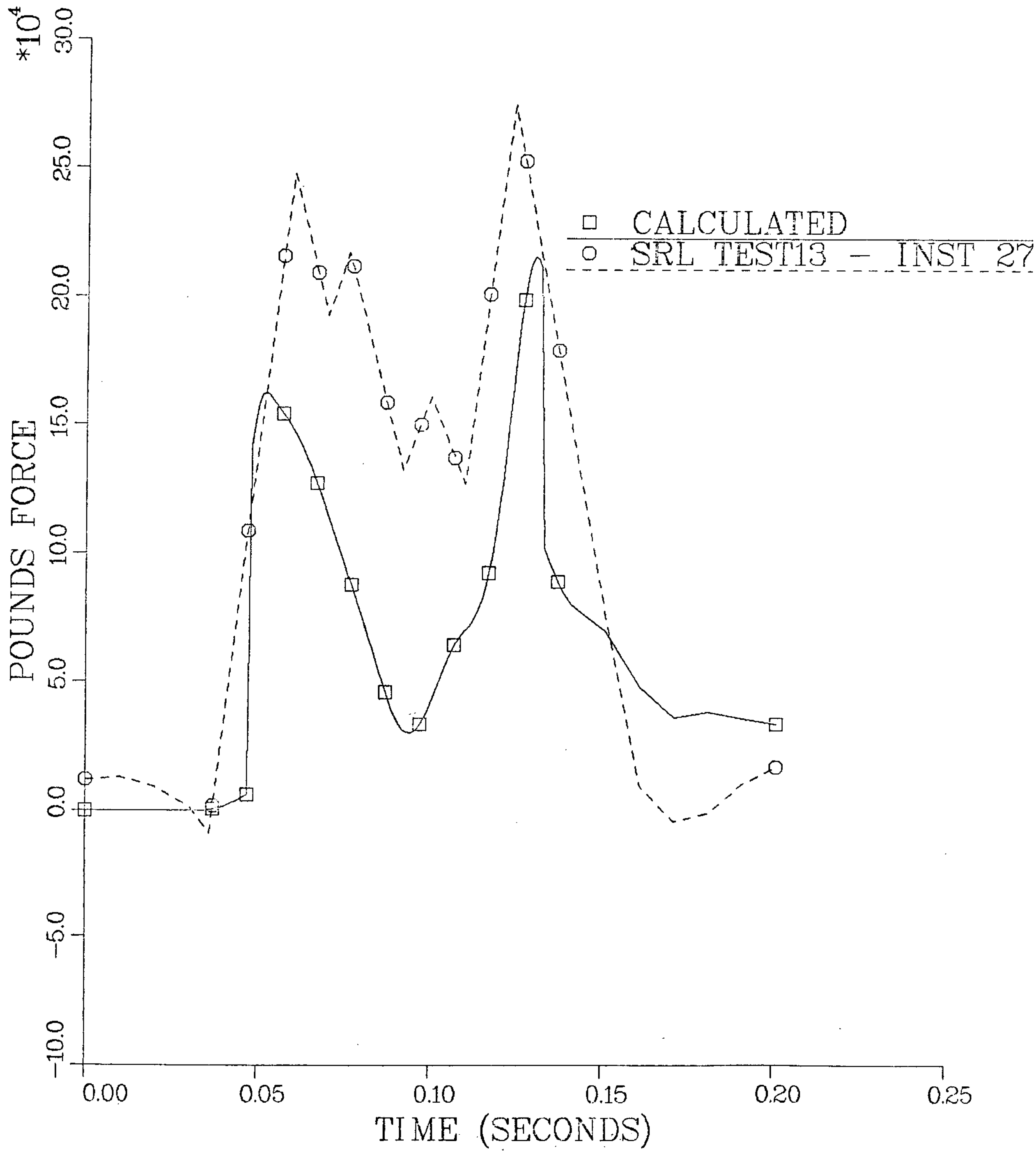

FIGURE 15. Horizontal Force of Interaction Between Cask and Rail Car vs Time During Impact with Four Hopper Cars Loaded with Ballast (Test 13 - Instruments 27 and 28).

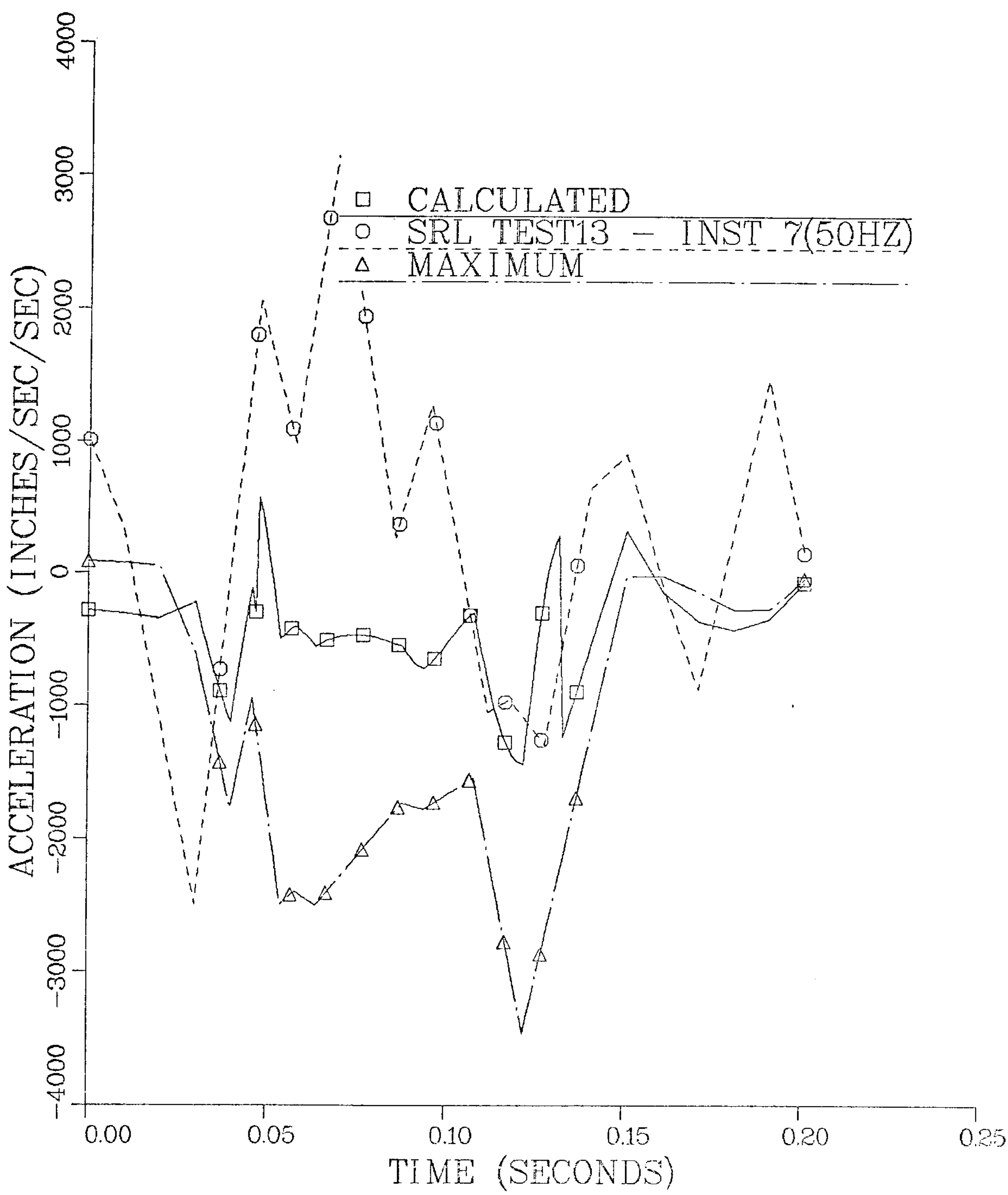

FIGURE 16. Horizontal Acceleration of the Cask-Rail Car During Impact with Four Hopper Cars Loaded with Ballast (Test 13 - Instrument 7: Filtered at 50 Hz).

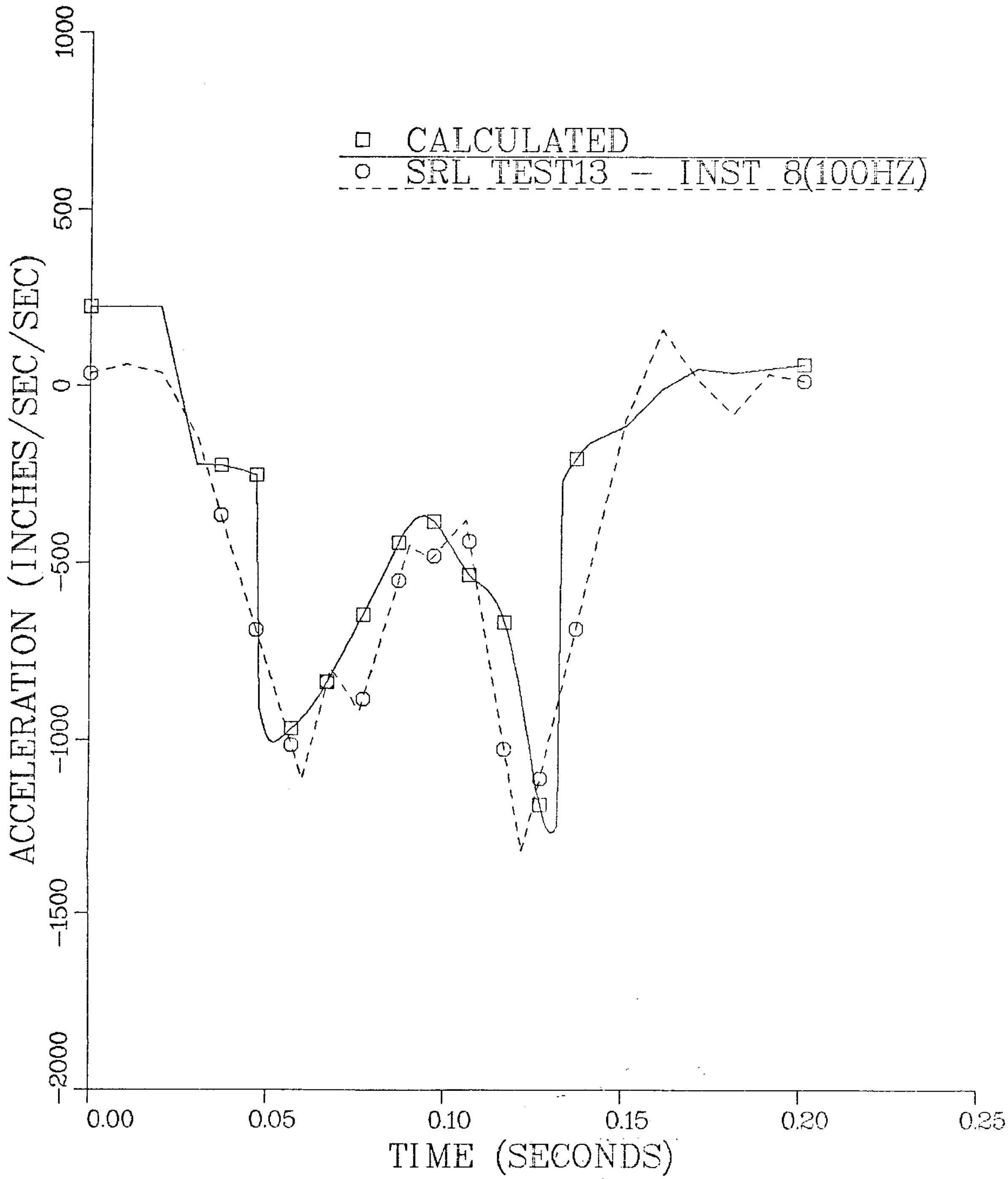

FIGURE 17. Horizontal Acceleration of the Cask During Impact with Four Hopper Cars Loaded with Ballast (Test 13 - Instrument 8: Filtered at 100 Hz).

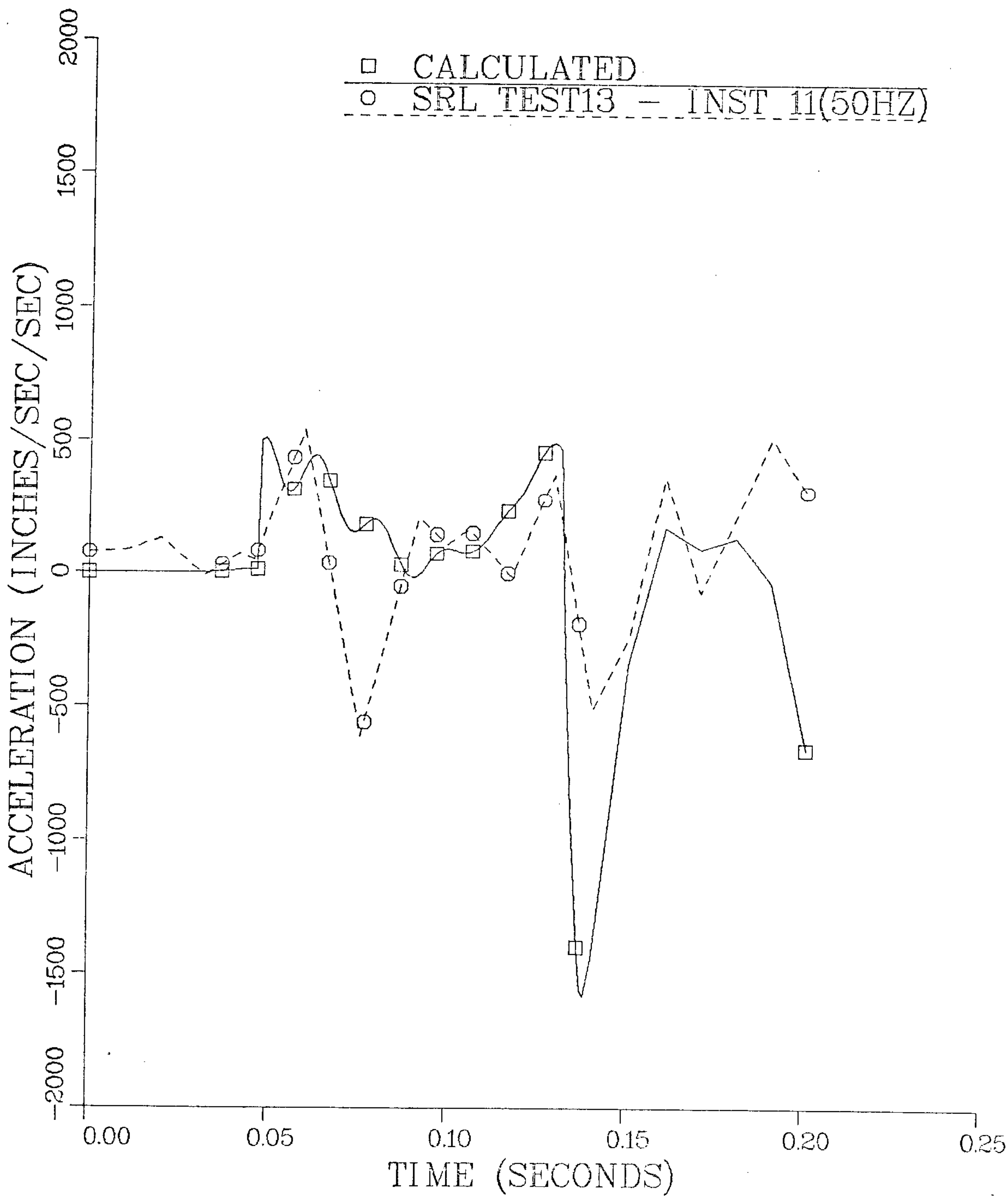

FIGURE 18. Vertical Acceleration of the Cask at the Far End During Impact with Four Hopper Cars Loaded with Ballast (Test 13 - Instrument 11: Filtered at 50 Hz).

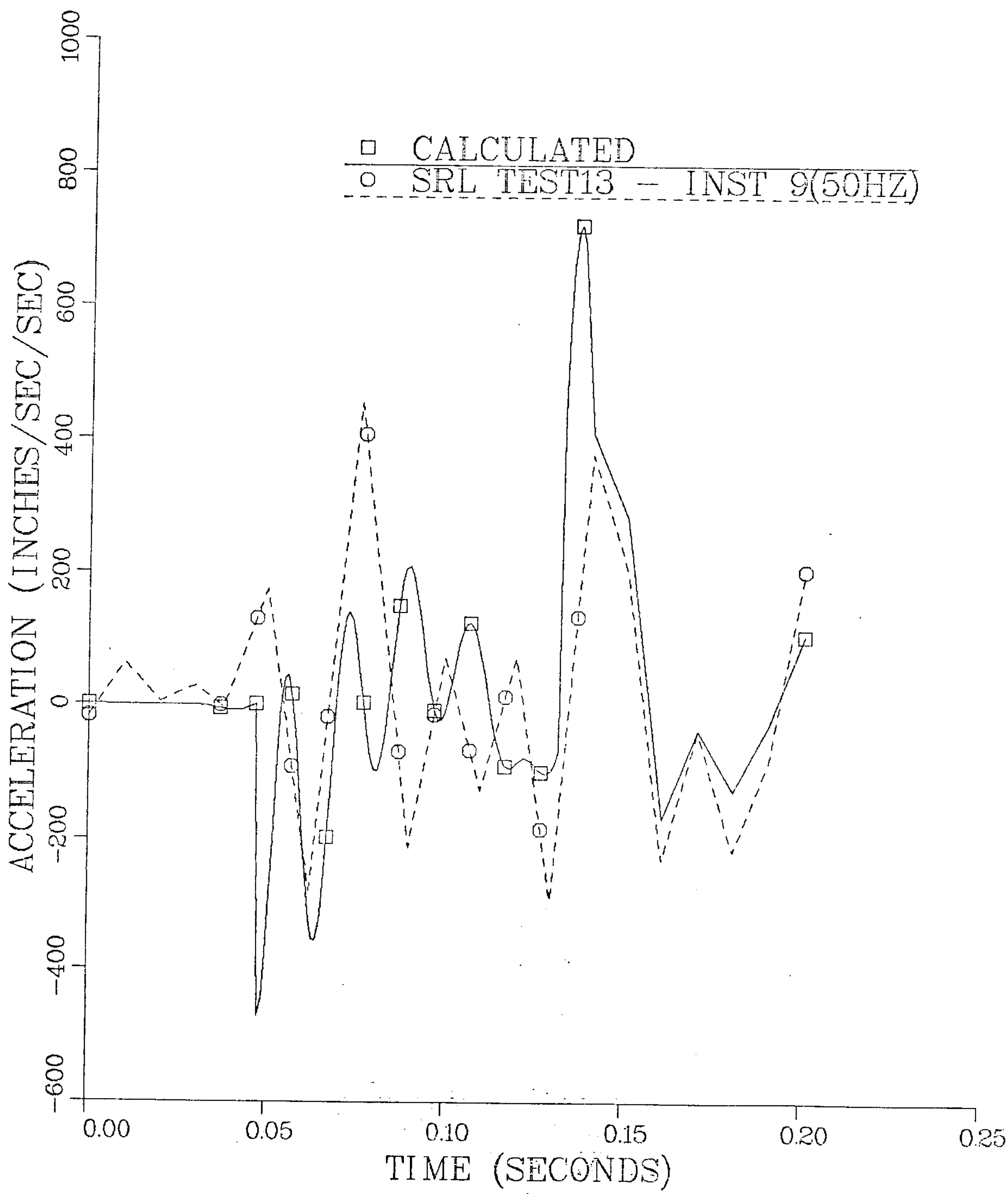

FIGURE 19. Vertical Acceleration of the Cask at the Struck End During Impact with Four Hopper Cars Loaded with Ballast (Test 13 - Instrument 9: Filtered at 50 Hz).

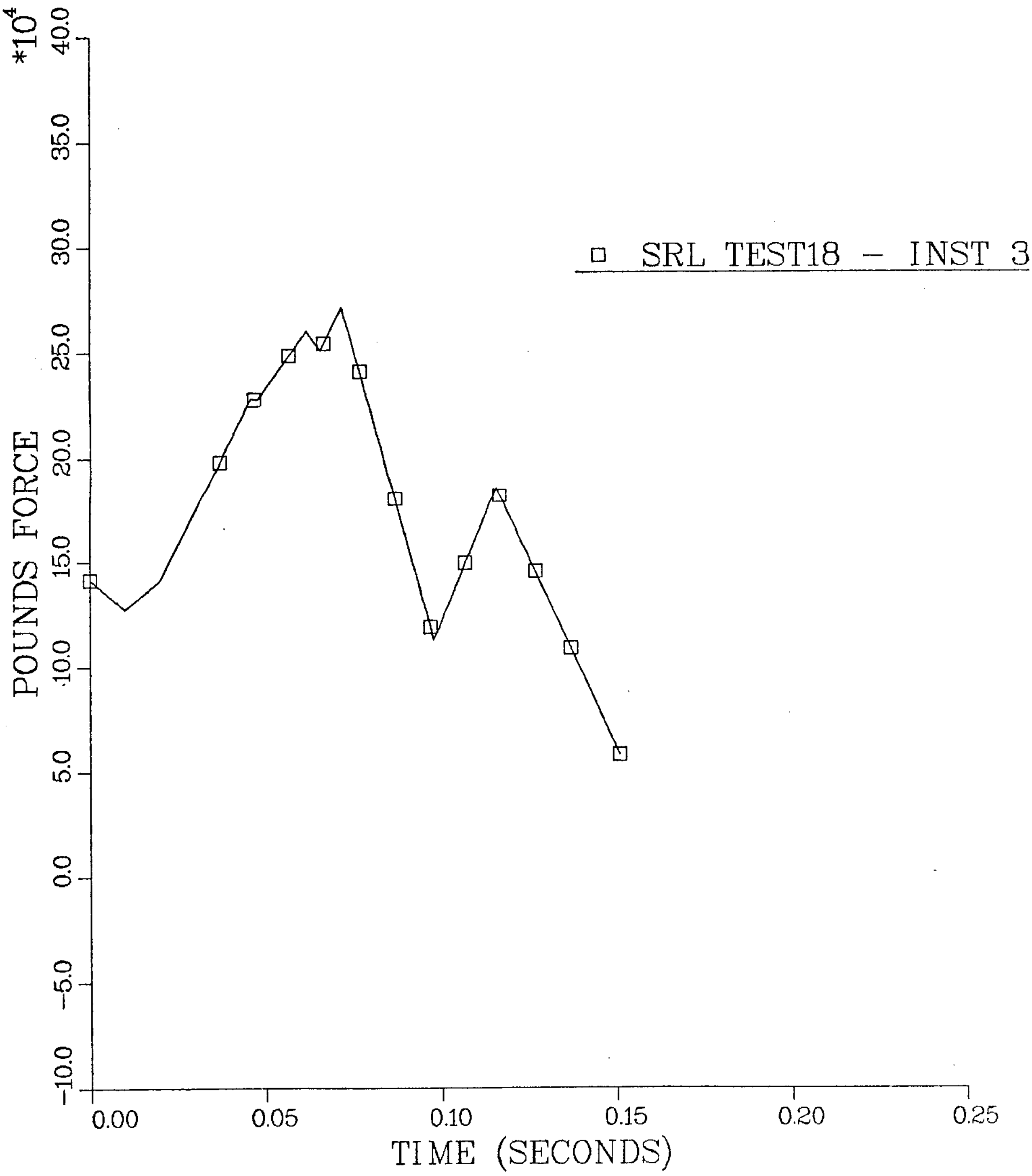

FIGURE 20. Coupler Force vs Time During Impact of Cask-Rail Car with Four Hopper Cars Loaded with Ballast (Test 18 - Instrument 3).

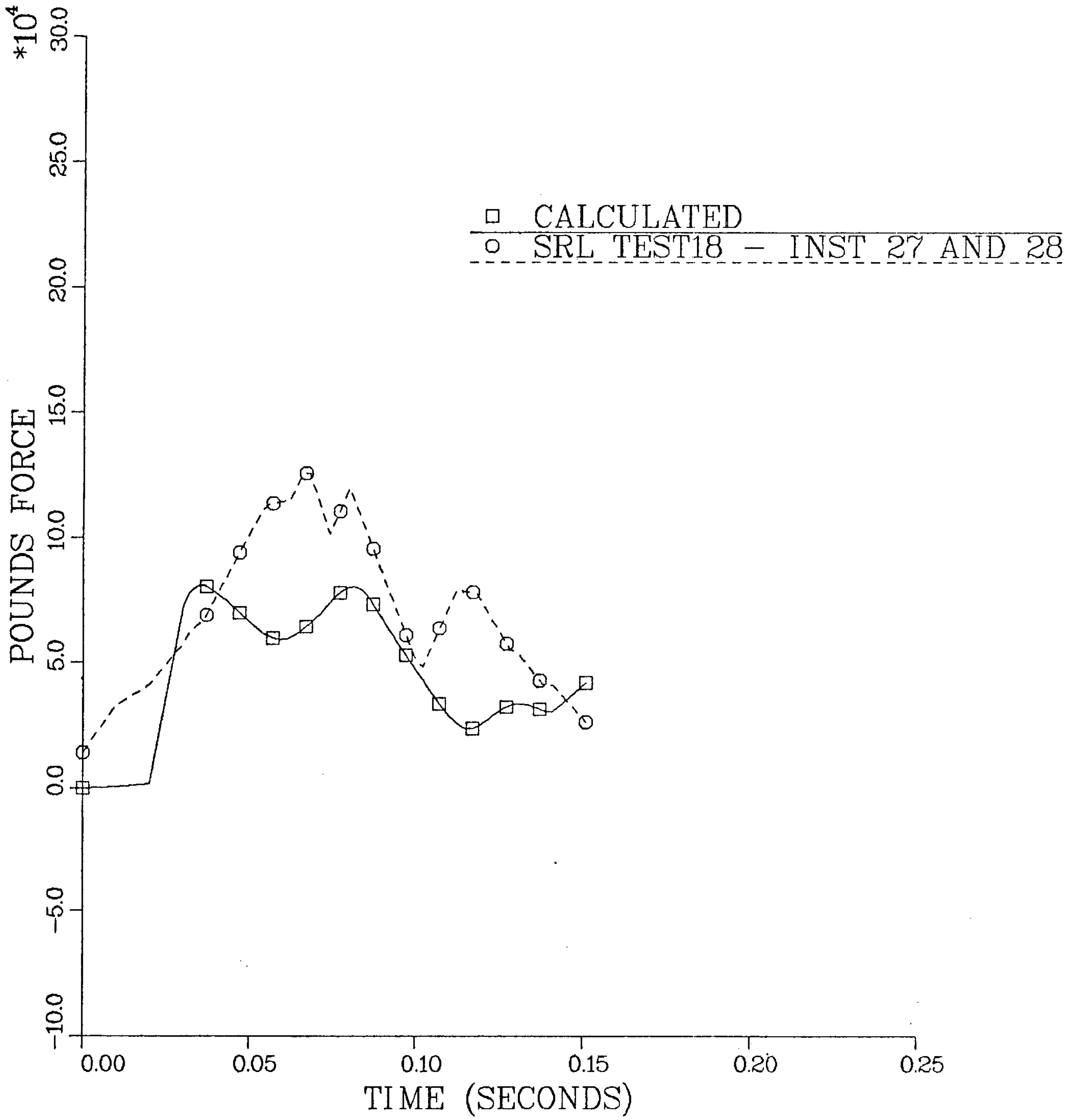

FIGURE 21. Horizontal Force of Interaction Between Cask and Rail Car vs Time During Impact with Four Hopper Cars Loaded with Ballast (Test 18 - Instruments 27 and 28).

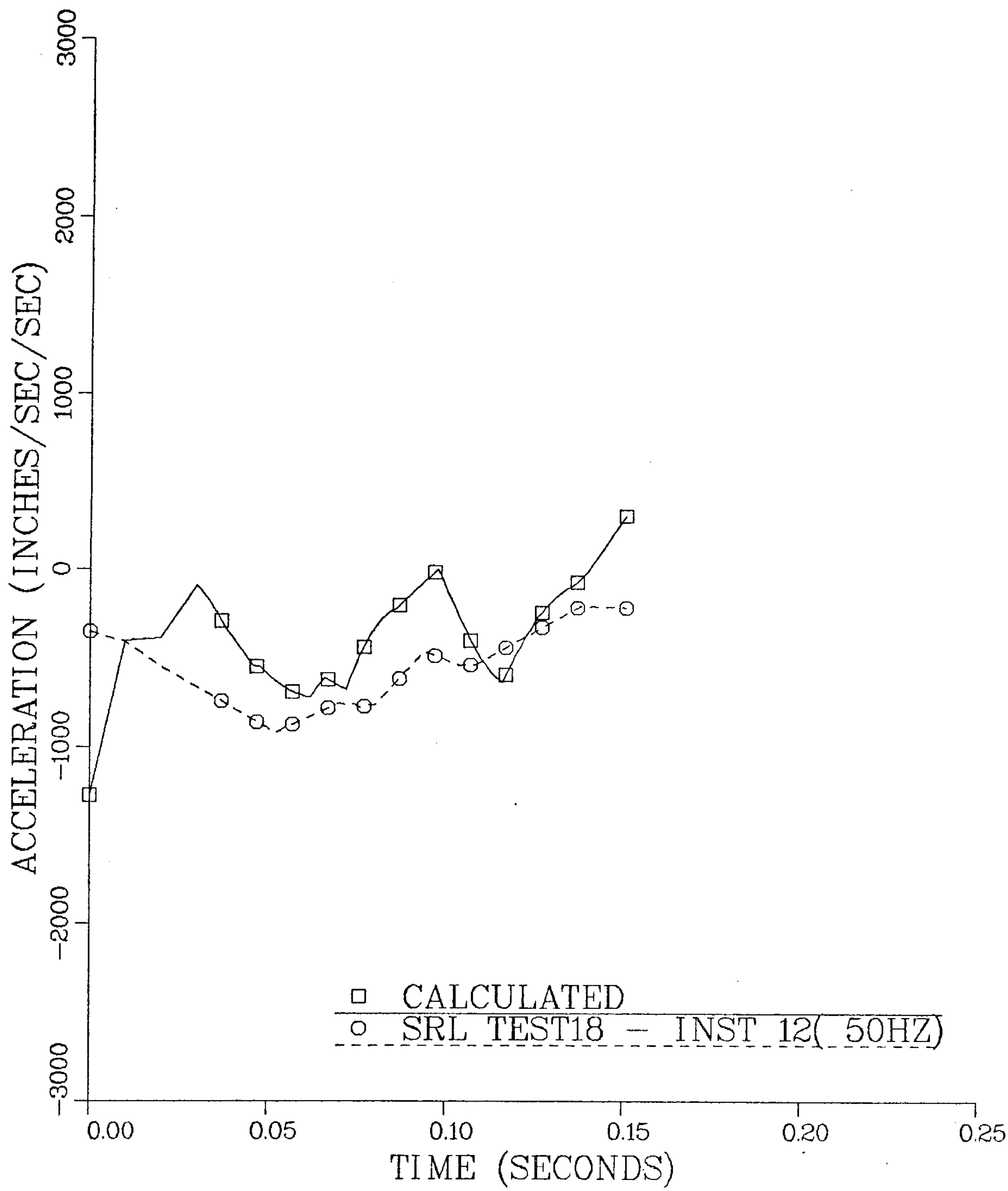

FIGURE 22. Horizontal Acceleration of the Cask-Rail Car During Impact with Four Hopper Cars Loaded with Ballast (Test 18 - Instrument 12: Filtered at 50 Hz).

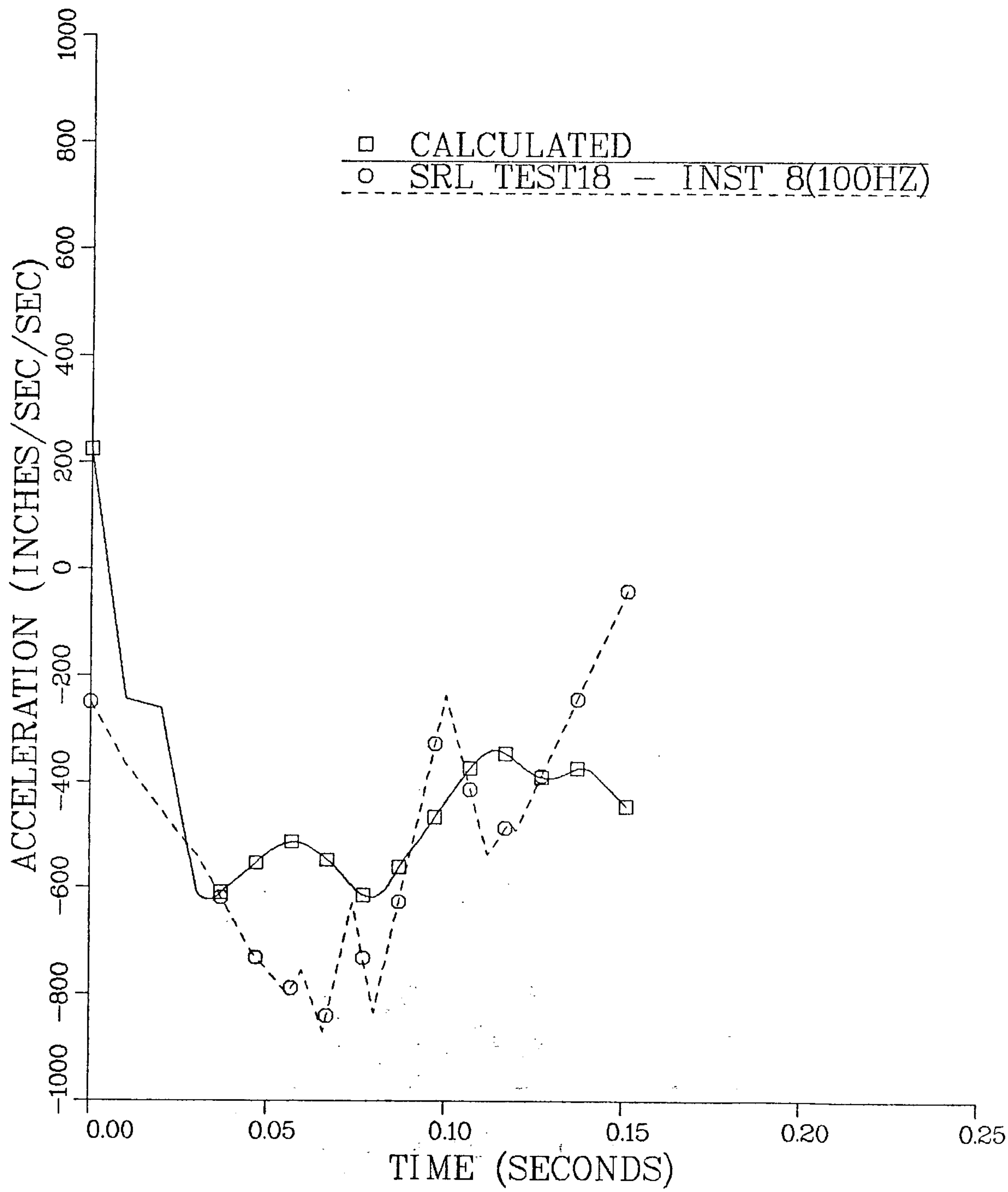

FIGURE 23. Horizontal Acceleration of the Cask During Impact with Four Hopper Cars Loaded with Ballast (Test 18 - Instrument 8: Filtered at 100 Hz).

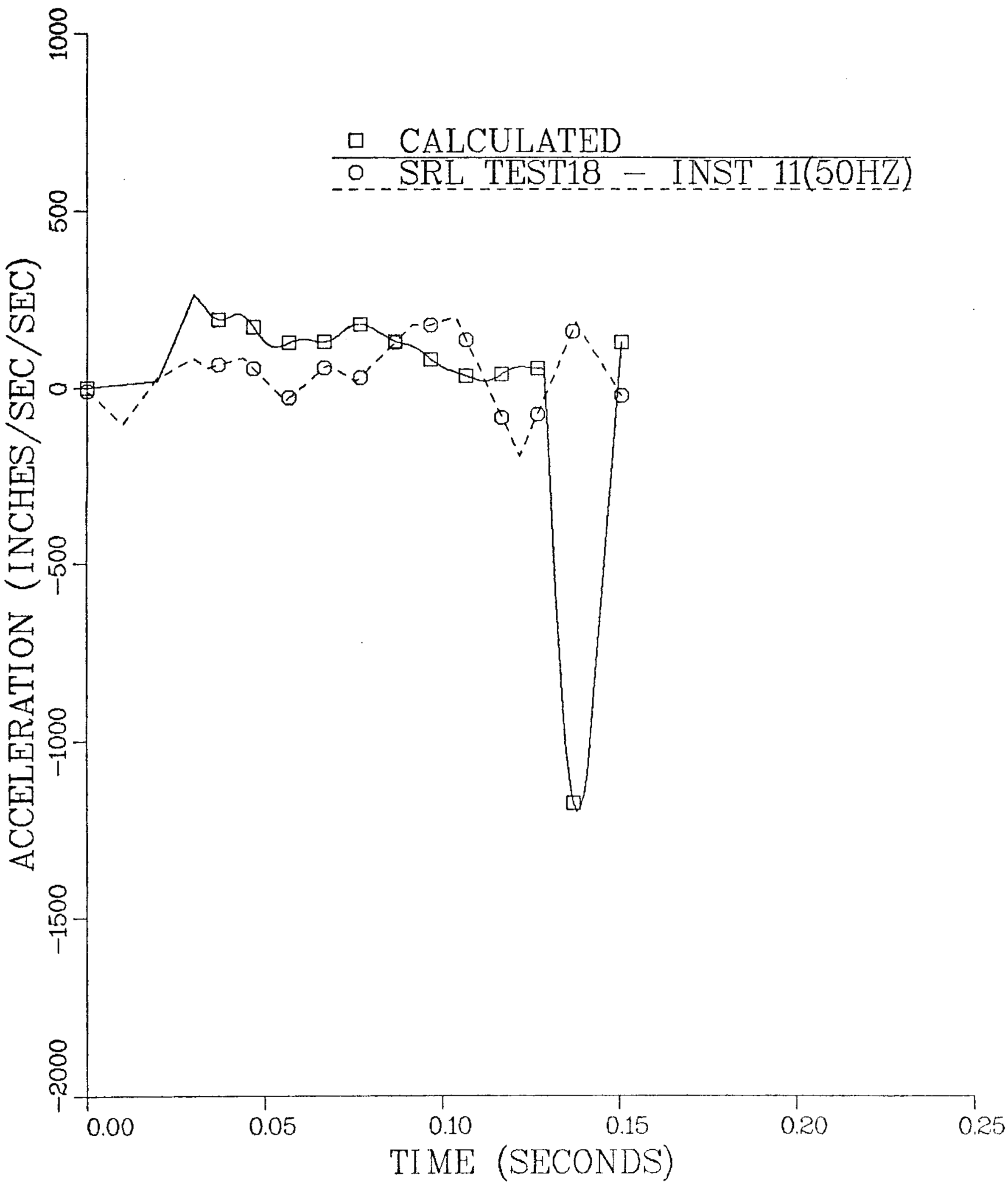

FIGURE 24. Vertical Acceleration of the Cask at the Far End During Impact with Four Hopper Cars Loaded with Ballast (Test 18 - Instrument 11: Filtered at 50 Hz).

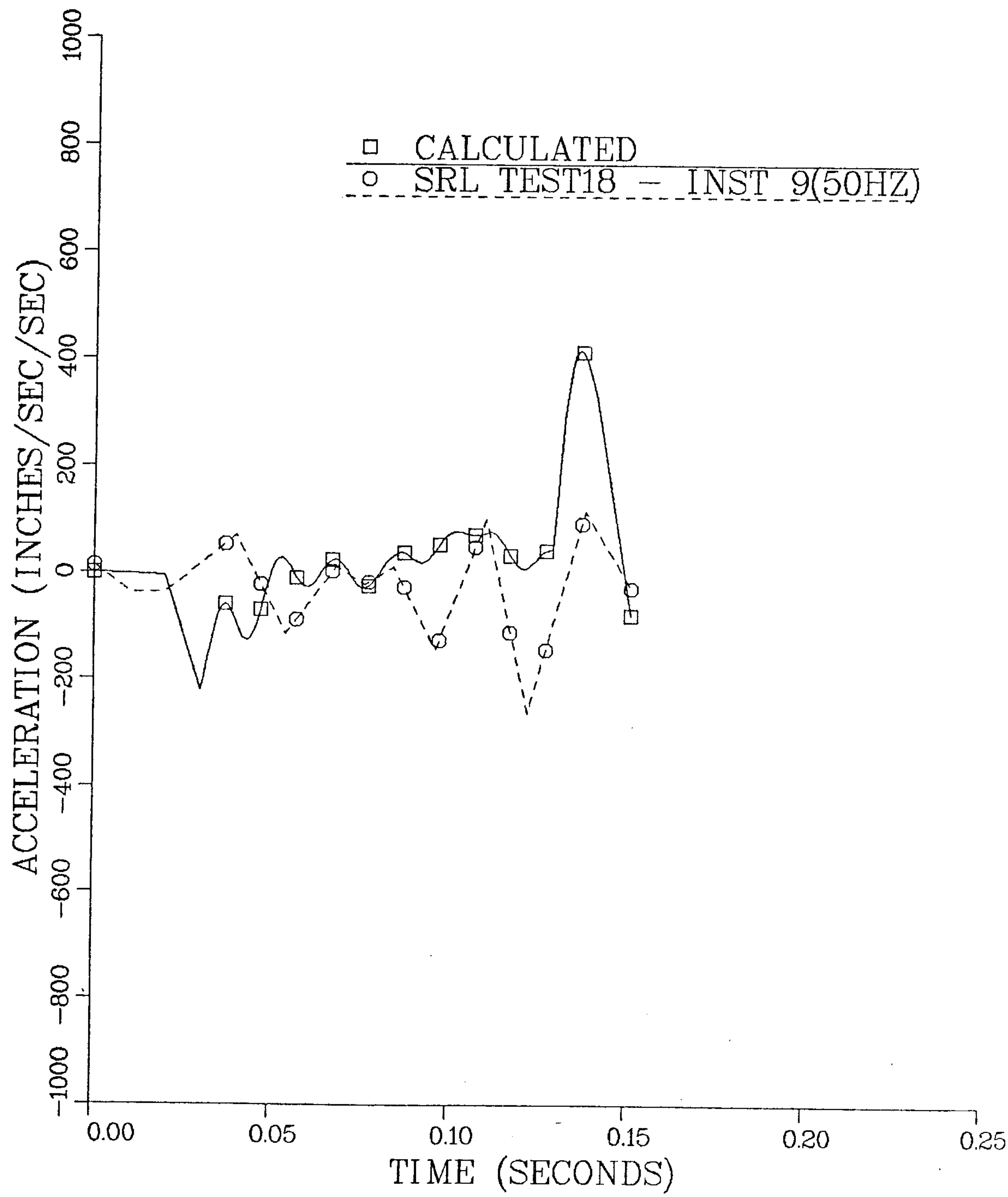

FIGURE 25. Vertical Acceleration of the Cask at the Struck End During Impact with Four Hopper Cars Loaded with Ballast (Test 18 - Instrument 9: Filtered at 50 Hz).

APPENDIX B

TABLES

TABLE 1

SUMMARY OF CONFIGURATIONS AND CONDITIONS OF COMPLETED CASK-RAIL CAR COUPLING TESTS

Test No.	Date	Rail Car	Coupler	Cask Wt (tons)	Impact Speed (mph)	Stop Frequency f_n	Tiedown	Remarks
								Preliminary Test Had No Instrumentation
P1	6/8	III	Std	42.5	5.5	-	-	- Concrete Simulation
P2	6/8	III	Std	42.5	7.6	-	-	- Welded Steel Stop - Cable Rigging to Restrain in Weight
P3	6/8	III	Std	42.5	11.8	-	-	- No Structural Damage
1	7/14	I	Std	40	8.3	Hi	A	Instrumented Coupler Faulty
2	7/18	I	Std	40	9.0	Hi	A*	Instrumented Coupler Faulty
3	7/19	I	Std	40	10.5	Hi	A	Instrumented Coupler Faulty
4	7/19	I	Std	40	10.7	Low	B	
5	7/20	I	Std	40	10.5	Hi	D	Cable Load Instruments Faulty
6	7/26	III	EOC	40	2.8	-	C	No Photography - No Data on Tape
7	7/26	III	EOC	40	5.6	-	C	No Photography - No Data on Tape
8	7/26	III	EOC	40	9.2	-	C	No Photography - No Data on Tape
9	7/26	III	EOC	40	9.2	-	C	No Photography - No Data on Tape
10	7/27	I	Std	70	8.0	-	A	One High Speed Camera Only
11	7/27	I	Std	70	11.2	-	A	One High Speed Camera Only
12	7/31	III	EOC	40	11.2	-	D	Data Questionable
13	8/1	III	EOC	40	11.2	-	D	Report of Test 12
14	8/1	III	Std	40	5.4	-	C	
15	8/1	III	Std	40	6.5	-	C	
16	8/2	III	Std	40	10.8	-	D	Some Cables Loose After Test
17	8/3	II	Cushion	40	5.9	-	D	
18	8/3	II	Cushion	40	10.7	-	D	

*Support Underbeam Reinforced (i.e., stiffened).

Key

Railcars:
- I 70 ton SCL - Std Couplers
- II 70 ton SCL - Cushion Underframe
- III 80 ton Union Carbide - Mixed Couplers

Tiedowns:
- A - 2 load cells between stop and cask bumper beams
  - 2 load bolts reproducibly snug
- B - Same as A, except f_n lowered with bumper beams
- C - Ten 1-in. cables at same angle - No stop
- D - Vertical Tiedown with six cables - two instrumented

DISTRIBUTION

RT (210)

DOE-RL/Office of Asst Manager
for Advanced Reactor Programs (2)
P. O. Box 550
Richland, WA 99352

EC Norman, Director, Technology Development Division
JJ Keating, Director, Breeder Technology Division

DOE/Chicago Patent Group
9800 South Cass Avenue
Argonne, IL 60439

AA Churm

DOE-HQ/Office of Operational Safety
EP-32
Washington, DC 20545

J. Counts

E. I. Du Pont DeNemours and Company
Savannah River Laboratory
Aiken, SC 29801

RH Towell

Los Alamos National Laboratory
P.O. Box 1663
Los Alamos, NM 87545

TD Butler

Battelle
Pacific Northwest Laboratory
P.O. Box 999
Richland, WA 99352

LD Williams

Sandia Laboratories
P.O. Box 5800
Albuquerque, NM 87185

CF Magnuson

HEDL (37)

HJ Anderson	W/C-28
JD Berger	W/E-12
AG Blasewitz	W/C-22
DA Cantley	W/A-4
RJ Cash	W/C-31
HA Carlson	W/C-28
MCJ Carlson	W/C-28
RE Dahl	W/C-22
JM Dahlke	W/C-115
AW DeMerschman	W/C-22
EA Evans	W/C-23
SR Fields (14)	W/C-28
RL Knecht	W/A-40
RE Lerch	W/C-35
SJ Mech	W/A-132
LH Rice	W/C-5
WE Roake	W/C-16
HH Yoshikawa	W/C-44
Central Files (3)	W/C-110
Publ Services (2)	W/C-115
Microfilm Services	W/C-123

NRC FORM 335 (7-77)

U.S. NUCLEAR REGULATORY COMMISSION

BIBLIOGRAPHIC DATA SHEET

1. REPORT NUMBER *(Assigned by DDC)* NUREG/CR-2146, Vol. 2 HEDL-TME 83-8	
4. TITLE AND SUBTITLE *(Add Volume No., if appropriate)* Dynamic Analysis to Establish Normal Shock and Vibration of Radioactive Material Shipping Packages Quarterly Progress Report April 1, 1981 - June 30, 1981	2. *(Leave blank)*
	3. RECIPIENT'S ACCESSION NO.
7. AUTHOR(S) S. R. Fields	5. DATE REPORT COMPLETED MONTH April YEAR 1983
9. PERFORMING ORGANIZATION NAME AND MAILING ADDRESS *(Include Zip Code)* Hanford Engineering Development Laboratory P.O. Box 1970 Richland, WA 99352	DATE REPORT ISSUED MONTH July YEAR 1983
	6. *(Leave blank)*
	8. *(Leave blank)*
12. SPONSORING ORGANIZATION NAME AND MAILING ADDRESS *(Include Zip Code)* Division of Risk Analysis Office of Nuclear Regulatory Research U.S. Nuclear Regulatory Commission Washington, DC 20555	10. PROJECT/TASK/WORK UNIT NO.
	11. CONTRACT NO. FIN B2263
13. TYPE OF REPORT Quarterly Progress Report	PERIOD COVERED *(Inclusive dates)* April 1, 1981 - June 30, 1981
15. SUPPLEMENTARY NOTES	14. *(Leave blank)*

16. ABSTRACT *(200 words or less)*

The CARDS (Cask Rail Car Dynamic Simulator) model was modified to simulate the cask-rail car systems used in Tests 13, 16 and 18 of the series of rail car coupling tests conducted at the Savannah River Laboratories (SRL) in July and August of 1978. An assessment of how well CARDS simulates the behavior of these cask-rail car systems was made by comparing calculated and experimental values of four response variables. This completes the development and validation of the CARDS model.

17. KEY WORDS AND DOCUMENT ANALYSIS

17a. DESCRIPTORS

17b. IDENTIFIERS/OPEN-ENDED TERMS

18. AVAILABILITY STATEMENT Unlimited	19. SECURITY CLASS *(This report)* Unclassified	21. NO. OF PAGES
	20. SECURITY CLASS *(This page)*	22. PRICE S

RC FORM 335 (7-77)

Availability of Reference Materials Cited in NRC Publications

Most documents cited in NRC publications will be available from one of the following sources:

1. The NRC Public Document Room, 1717 H Street, N.W.
   Washington, DC 20555

2. The NRC/GPO Sales Program, U.S. Nuclear Regulatory Commission,
   Washington, DC 20555

3. The National Technical Information Service, Springfield, VA 22161

Although the listing that follows represents the majority of documents cited in NRC publications, it is not intended to be exhaustive.

Referenced documents available for inspection and copying for a fee from the NRC Public Document Room include NRC correspondence and internal NRC memoranda; NRC Office of Inspection and Enforcement bulletins, circulars, information notices, inspection and investigation notices; Licensee Event Reports; vendor reports and correspondence; Commission papers; and applicant and licensee documents and correspondence.

The following documents in the NUREG series are available for purchase from the NRC/GPO Sales Program: formal NRC staff and contractor reports, NRC-sponsored conference proceedings, and NRC booklets and brochures. Also available are Regulatory Guides, NRC regulations in the *Code of Federal Regulations,* and *Nuclear Regulatory Commission Issuances.*

Documents available from the National Technical Information Service include NUREG series reports and technical reports prepared by other federal agencies and reports prepared by the Atomic Energy Commission, forerunner agency to the Nuclear Regulatory Commission.

Documents available from public and special technical libraries include all open literature items, such as books, journal and periodical articles, and transactions. *Federal Register* notices, federal and state legislation, and congressional reports can usually be obtained from these libraries.

Documents such as theses, dissertations, foreign reports and translations, and non-NRC conference proceedings are available for purchase from the organization sponsoring the publication cited.

Single copies of NRC draft reports are available free upon written request to the Division of Technical Information and Document Control, U.S. Nuclear Regulatory Commission, Washington, DC 20555.

Copies of industry codes and standards used in a substantive manner in the NRC regulatory process are maintained at the NRC Library, 7920 Norfolk Avenue, Bethesda, Maryland, and are available there for reference use by the public. Codes and standards are usually copyrighted and may be purchased from the originating organization or, if they are American National Standards, from the American National Standards Institute, 1430 Broadway, New York, NY 10018.

GPO Printed copy price: $4.25